Geomorphology 125 (2011) 541–557

Contents lists available at ScienceDirect

Geomorphology

journal homepage: www.elsevier.com/locate/geomorph

Beryllium-10 terrestrial cosmogenic nuclide surface exposure dating of Quaternary landforms in Death Valley

Lewis A. Owen [a,*], Kurt L. Frankel [b], Jeffrey R. Knott [c], Scott Reynhout [a], Robert C. Finkel [d,e], James F. Dolan [f], Jeffrey Lee [g]

[a] Department of Geology, University of Cincinnati, Cincinnati, Ohio, USA
[b] School of Earth and Atmospheric Sciences, Georgia Institute of Technology, Atlanta, GA 30332, USA
[c] Department of Geological Sciences, California State University, Fullerton, California, USA
[d] Department of Earth and Planetary Science Department, University of California, Berkeley, Berkeley, CA 94720-4767, USA
[e] CEREGE, BP 80 Europole Méditerranéen de l'Arbois, 13545 Aix en Provence Cedex 4, France
[f] Department of Earth Sciences, University of Southern California, Los Angeles, California, USA
[g] Department of Geological Sciences, Central Washington University, Ellensburg, Washington, USA

ARTICLE INFO

Article history:
Received 10 March 2010
Received in revised form 3 October 2010
Accepted 18 October 2010
Available online 26 October 2010

Keywords:
Death Valley
Terrestrial cosmogenic nuclides
Optically stimulated luminescence
Alluvial fans
Shore lines
Lake Manly

ABSTRACT

Quaternary alluvial fans, and shorelines, spits and beach bars were dated using ^{10}Be terrestrial cosmogenic nuclide (TCN) surface exposure methods in Death Valley. The ^{10}Be TCN ages show considerable variance on individual surfaces. Samples collected in the active channels date from ~6 ka to ~93 ka, showing that there is significant ^{10}Be TCN inheritance within cobbles and boulders. This suggests that the predominantly bedrock hillslopes erode very slowly and sediment is transferred very gradually in most regions within Death Valley. Comparisons of ^{10}Be TCN ages on alluvial fan surfaces with chronostratigraphies based on soil development and optically stimulated luminescence dating show that minimum ^{10}Be TCN ages within sample sets on individual surfaces most closely approximate to the age of landforms that are younger than ~70 ka. Alluvial fan surfaces older than ~70 ka have begun to undergo sufficient erosion such that the majority of ^{10}Be TCN ages for datasets on individual surfaces probably underestimate the true age of the surface due to erosion and exhumation of fresh cobbles and boulders. The spread of ^{10}Be TCN ages for beach bars near Beatty Junction and shorelines ~8 km south of Furnace Creek is large, ranging from ~119 ka to ~385 ka and ~109 ka to ~465 ka, respectively. New and previously published luminescence ages and soil development suggest that these landforms may have formed during marine isotope stage (MIS) 2 (~22–18 ka), but these younger ages may reflect elluviation of material into the bar deposit long after deposition, and hence the younger ages do not record the true antiquity of the landforms. This disparity between dates determined by different dating methods and the large spread of TCN ages suggests that the cobbles and boulders have considerable inherited ^{10}Be concentrations, suggesting that the clasts have been derived from older shorelines or associated landforms. These results highlight the problems associated with using surface cobbles and boulders to date Quaternary surfaces in Death Valley and emphasizes the need to combine multiple, different dating methods to accurately date landforms in similar dryland regions elsewhere in the world. However, these results highlight the potential to use TCN methods, when used in combination with other dating techniques, to examine and quantify processes such as sediment transfer and denudation in drylands.

1. Introduction

Death Valley constitutes one of the most dramatic landscapes in North America, and is famous for its faulted mountain fronts, spectacular alluvial fans, and extensive saline playa. The valley is recognized for being the hottest (maximum recorded temperatures of 56.7 °C at Furnace Creek on July 13, 1913), driest, and lowest location (85.5 m below sea level at Badwater) in North America. In February 1933, President Herbert Hoover made Death Valley a National Monument, and it was designated a biosphere reserve in 1984, and became a U.S. National Park in 1994.

Despite its fame and environmental significance, relatively little work has been undertaken to date landforms in Death Valley. This is partially because of the difficulty in defining the ages of landforms by the standard technique of radiocarbon dating due to the absence of organic matter in sediments. Nevertheless, relative ages of landforms have been determined by numerous researchers using a combination of morphological, relative weathering and soil characteristics (Denny,

* Corresponding author. Tel./fax: +1 513 556 4203.
E-mail address: lewis.owen@uc.edu (L.A. Owen).

0169-555X/$ – see front matter © 2010 Elsevier B.V. All rights reserved.
doi:10.1016/j.geomorph.2010.10.024

1965; Hunt and Mabey, 1966; Bull, 1968; Hooke, 1972; McFadden et al., 1989, 1991; Hooke and Dorn, 1992; Nishiizumi et al., 1993; Ku et al., 1998; Machette et al., 2001, 2008; Klinger, 2001a,b,c,d; Klinger and Piety, 2001; Knott et al., 2005; Frankel and Dolan, 2007). In recent years, however, the developing methods of optically stimulated luminescence (OSL) and terrestrial cosmogenic nuclide (TCN) surface exposure dating have allowed many landforms to be dated within the valley (Frankel et al., 2007a; Machette et al., 2008; Frankel et al., 2010a,b). Successful application of these methods requires detailed considerations of the geomorphic, climatic, and tectonic origin of the landforms that are being dated, as well as an understanding of the theory, chemistry, and physics behind the methods that are applied to avoid misinterpreting ages.

As part of a larger study to determine slip rates on the Death Valley–Fish Lake Valley fault system that bounds the northwestern edge of the valley, we undertook an intensive program of ^{10}Be TCN and OSL dating, which included determining >70 ^{10}Be TCN and ~30 OSL ages on landforms throughout Death Valley (Frankel et al., 2007a, 2010a,b). In this paper, we utilize many of these data and report an additional 44 new ^{10}Be TCN and two new OSL dates to determine ages for selected landforms in Death Valley. We then assess the methods and problems associated with the application of ^{10}Be TCN methods in this region and similar environments.

The application of TCN methods can prove problematic since the TCN ages on surface clasts (pebbles, cobbles, and boulders) may provide significant over-estimates of the true age of the landforms if the clasts have acquired substantial TCN concentrations prior to final deposition (inheritance). Alternatively, TCN ages on rock surfaces might under-estimate the true age of the landform if the rock surface or clast has been recently exhumed or weathered. Various methods, such as determining multiple ages on surfaces and analyzing TCN depth profiles, have been used to help assess these problems. Most presume that these geologic processes are stochastic and that when ages cluster, these processes have not significantly affected TCN concentrations and that the model ages reflect the true age of the landforms. However, defining 'significant clustering' of ages and/or the age within a distribution that most accurately represents the true landform age can be very subjective. Here, we examine these problems and highlight the limitations of applying these methods in Death Valley specifically, and drylands in general.

2. Regional setting

Death Valley is located along the western margin of the Great Basin in the southwestern USA (Fig. 1). The valley is an oblique pull-apart basin in the transition between the extensional Basin and Range Province and the right-lateral strike-slip faults comprising the eastern California shear zone (Burchfiel and Stewart, 1966). The valley has formed since the Miocene by displacement along a down-to-the-west normal fault in a step-over between the dextral southern Death Valley and northern Death Valley fault zones (Burchfiel and Stewart, 1966; Hamilton, 1988; Wernicke et al., 1988; Burchfiel et al., 1995; Miller and Pavlis, 2005). Death Valley is bounded by the Cottonwood and Panamint Mountains, and Last Chance Range to the west; and the Grapevine, Funeral and Black Mountains to the east. The Panamint Mountains rise >3000 m above sea level (asl), to the highest point, Telescope Peak, at 3368 m asl. The bedrock is very diverse, ranging in age from Proterozoic to Cenozoic, and includes metamorphic crystalline basement, dolomites, limestones, quartzite, sedimentary siliclastics and volcanic ashes (Hunt and Mabey, 1966).

The present-day arid climate results from the rain shadow produced by the Sierra Nevada, Inyo Mountains, and Panamint Mountains (Poage and Chamberlain, 2002). From 1961 to 2008 the weather station at Furnace Creek in the central part of Death Valley recorded an average yearly temperature of 24.8 °C with an average high in January and July of ~19 °C and ~47 °C, respectively, and an average annual precipitation of 57 mm (Western Regional Climate Center, 2010). Geochemical and sedimentological analysis of sediment cores show that the late Quaternary climate was dominated by two wet, cold periods and two warm, dry intervals (Li et al., 1996; Lowenstein et al., 1999). The evidence suggests that perennial lakes existed in the central basin during the penultimate glacial advance from ~128 to 186 ka and during the last glacial maximum from ~12 to 35 ka when the climate was cooler and wetter (Lowenstein et al., 1999).

The gross geomorphology of Death Valley can be broadly divided into three physiographic provinces: the playa floor of the valley; extensive alluvial fans that form a bajada along valley-bounding range fronts; and steep, long, essentially bare bedrock hillslopes that rise to high mountain peaks and are incised by deep canyons. The alluvial fans of Death Valley are commonly featured in textbooks as classic examples and were examined during some of the early, seminal work on these landforms (e.g., Bull, 1968). Owing to its position below sea level, the valley is internally drained and the fluvial source is the Amargosa River.

3. Previous work

The long history of Quaternary geology and geomorphology research in Death Valley began with observations by Gilbert (1890), who recognized ancient shorelines along the Black Mountains and suggested a large lake once occupied the region. These observations were expanded on by Nobel (1926), who noted several lake-shore terraces upon a basalt hill near the southern end of Death Valley, a feature now known as Shoreline Butte. The first extensive study of Death Valley was undertaken by Blackwelder (1933) who described the evidence for the lake recognized by Gilbert (1890), coining the name Lake Manly in honor of W.L. Manly who led, and heroically rescued, the first party of western emigrants who entered Death Valley in 1849 (Means, 1932).

Modern geomorphic research in Death Valley began with focus on the widespread alluvial fans as a keystone for the Quaternary stratigraphy of the valley and arid regions throughout western North America (Denny, 1965; Hunt and Mabey, 1966). This work continued both in Death Valley and throughout southwestern North America, resulting in a relatively consistent alluvial fan stratigraphy for the region; however, subtle differences in the nomenclature exist between researchers, as illustrated in Table 1 (Denny, 1965; Hunt and Mabey, 1966; Reynolds, 1969; Hooke, 1972; Moring, 1986; Bull, 1991; Hooke and Dorn, 1992; Nishiizumi et al., 1993; Klinger, 2001a,d; Frankel and Dolan, 2007; Machette et al., 2001, 2008). From the late 1980s to the early 2000s, a series of detailed studies of the Quaternary geology and geomorphology was undertaken that resulted in a string of doctoral theses, field guides, and USGS publications (e.g., Troxel, 1986; Knott, 1998; Anderson, 1998; Professional Soil Scientists Association of California, 1998; Wright and Troxel, 1999; Klinger, 2001a,b,c,d; Machette et al., 2001).

Sohn et al. (2007) undertook the first comprehensive OSL dating study of Quaternary landforms in Death Valley. This work showed that Q3b alluvial fan deposits have OSL ages from ~4 to ~7 ka, Q3a alluvial fan deposits have OSL ages from ~11 to ~17 ka, and Q2d alluvial fan deposits have OSL ages of ~25 ka along the eastern Black Mountains piedmont.

Zreda (1991, cited in Orme and Orme, 1991), Trull et al. (1995), Nishiizumi et al. (1993), and Phillips and Zreda (1999) determined the first TCN ages in Death Valley using ^{36}Cl, ^{26}Al, ^{10}Be, and ^{3}He to date lake and alluvial fan features. Knott (unpublished data, 1998) followed this study by dating a landslide deposit along the western Black Mountains using ^{10}Be methods. Next, Frankel et al. (2007a) provided the first comprehensive study using TCNs for Death Valley, focusing on dating faulted alluvial fans using both ^{36}Cl and ^{10}Be. Recently, Machette et al. (2008) used ^{36}Cl TCNs in 12 depth profiles to establish the age of some of the most extensive Quaternary alluvial

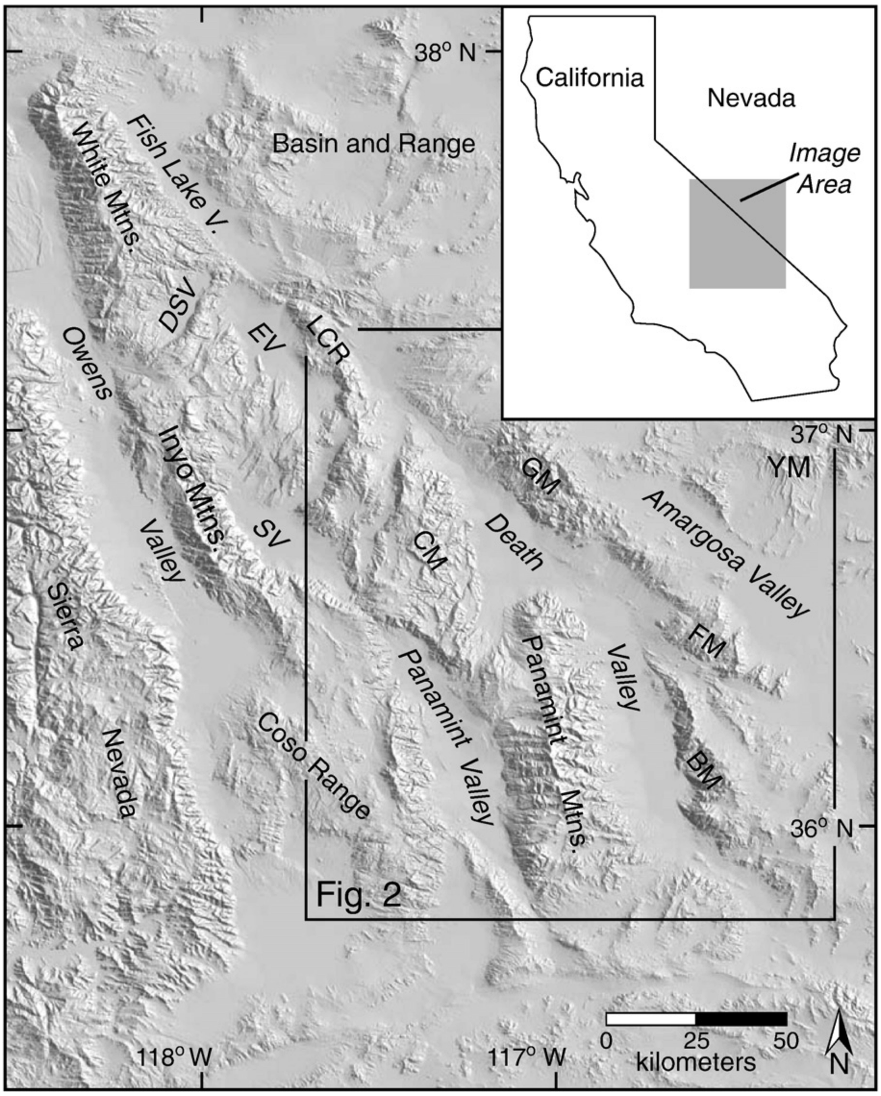

Fig. 1. Regional location/setting for Death Valley (BM – Black Mountains; CM – Cottonwood Mountains; DSV – Deep Springs Valley; EV – Eureka Valley; FM – Funeral Mountains; GM - Grapevine Mountains; LCR – Last Chance Range; SV – Saline Valley; YM – Yucca Mountain).

fans in Death Valley. Their intermediate-age (Qai) alluvial fans ranged from ~40 to 100 ka, with a mean age of ~70 ka, and an older phase of alluvial-fan deposits (Qao) were dated to ~170 ka. In addition, Frankel et al. (2007b) and Ganev et al. (2010) determined ^{10}Be on four offset alluvial fans in Fish Lake Valley showing that the fans range from ~71 ka to ~121 ka. Frankel et al. (2010a,b) dated Holocene alluvial fans near Badwater and at Mormon Point and a late Pleistocene alluvial fan south of Mud Canyon, which will be discussed in more detail below.

4. Methods

Seven study areas were chosen to examine the characteristics of some classic landforms in Death Valley, which included alluvial fans, active channels, and shorelines, spits and beach bars of Lake Manly (Fig. 1). Several of the study areas provided useful data for defining rates of displacement along the Death Valley–Fish Lake fault zone. The results of these tectonic geomorphic studies are described in Frankel et al. (2007a, 2010a,b).

Landforms were mapped in the field on base maps produced from high-resolution airborne LiDAR digital topographic data. The detailed processing of the LiDAR data is described in Frankel et al. (2007b). We use the fan characteristics defined by Bull (1991) and nomenclature of Klinger (2001a) to define the Quaternary stratigraphic units in our study area (Table 1). Samples for ^{10}Be TCN dating were collected from surfaces within each of the study areas to help define the ages of landforms and to test the applicability of the method. In addition two OSL samples were collected from one of the Lake Manly beach bars ~8 km south of Furnace Creek.

4.1. Be-10 terrestrial cosmogenic dating

Samples were collected from surface boulders and cobbles for ^{10}Be TCN dating. Where possible, large boulders (>1 m high) were preferentially sampled from sites that showed the least evidence of erosion. For surface boulders ~250 g of rock was chiseled off the upper ≤5 cm surface. Whole cobbles were collected where boulders were absent. The location, geomorphic setting, size, shape, and weathering characteristics of each sample were recorded and are listed in Table 2. The inclination from the sampling site to the surrounding horizon was measured to quantify topographic shielding, which in most locations was negligible.

Boulder and cobble samples were crushed and sieved to obtain a 250–500 μm grain size fraction. The 250–500 μm size fraction was

Table 1
Correlation of Quaternary stratigraphic units in Death Valley (adapted from Klinger, 2001d and Machette et al., 2008); and generalized descriptions for Late Quaternary stratigraphic units (after Klinger, 2001b).

	Denny, 1965	Hunt and Mabey, 1966	Reynolds, 1969	Hooke, 1972[1]	Moring, 1986	Bull, 1991[2]	Hooke and Dorn, 1992	Nishiizumi et al., 1993[2]	Klinger, 2001a; Frankel and Dolan, 2007	Machette et al., 2008	Desert pavement[4]	Bar/swale morphology[5]	Rock varnish[6]	Soil characteristics[7]: profile development; Profile thickness (cm); maximum profile color
Holocene			Q1	Qa	Qf4/Qs	Q4b			Q4b		None	Prominent	None	None; None; 10YR6/3
	Qgv	Qg4		Qai	Qmu	Q4a	Q4		Q4a	Qay	None	Prominent	None	Thin Av/2C; 4; 10YR7/2
			Q2			Q3c			Q3c		PP	Distinct	5YR6/6	Avk/2Bkz/2C; 20; 10YR7/3
	Qgv	Qg3		Qat	Qf3	Q3b			Q3b	Qayo	MP	Subdued	5YR5/8	Avk/2Bkz/2C; 50; 10YR7/3
			Q3			Q3a			Q3a	Qai	MP-WP	Subdued	5YR5/8 to 2.5YR4/8	Avk/Bkz/2C; 72; 10YR6/4
									Qlm4/Qlr					
		Q1m			Qf2c	Q2c			Q2c		WP	None	2.5YR4/8	Avkz/Btkz/2Bz; 100; 7.5YR5/6
Pleistocene				Qay	Q1		Q3	3a		Qaio				
	Qgp	Qg2	Q4		Qf2b	Q2b			Q2b					
				Qai	Qf2a		Q2	2a	Qlm3	Qao				
						Q2a			Q2a					
									Qlm2					
				Qao		Q1	Q1	1a	Q1c	QTa				
					Qf1									
									Q1b					
		QTg1												
Pliocene									Qlml					
					Tg/Tb				QT1a					
		Tfc												

[1]Hooke (1972), his Fig. 4B) did not label his units, but patterned them according to facies and subdivided them (that is, active, inactive, trans., young, intermediate, and old). The map unit symbols shown above are based on his explanation for channel facies (Qc) deposits: a is active, i is inactive, and t is transitional to Lake Manly deposits. For surface facies (Qs) deposits: y is younger, i is intermediate, and o is older.
[2]Original classification was based on the Lower Colorado River region, but applied regionally and specifically in Death Valley.
[3]Geologic map units based on Dorn (1988).
[4]Desert pavement development is rated on the basis of stone packing on the pavement surface and is dependent upon particle size and clast shape of the original deposit: PP, poorly-packed; MP, moderately packed; WP, well-packed.
[5]Bar-and-swale morphology as a relative measure of the original depositional topography and its degree of preservation.
[6]Maximum rubification color on the bottom of clasts in the pavement using Munsell color notation.
[7]Typical profile development; described in the field as outlined by the Soil Survey Division Staff (1993) and by Birkeland (1999). Maximum profile thickness observed. Dry color on <2 mm soil fraction using Munsell color notation.

processed using four acid leaches: aqua regia for >9 h, two 5% HF/HNO_3 leaches for ~24 h, and one 1% HF/HNO_3 leach for 24 h. Lithium heteropolytungstate heavy liquid separation was applied after the first 5% HF/HNO_3 leach. Be carrier was added to the pure quartz. The quartz was dissolved in 49% HF and HNO_3, fumed with perchloric acid, and passed through anion and cation exchange columns along with chemical blanks to extract $Be(OH)_2$. The $Be(OH)_2$ was oxidized to BeO through ignition at 750 °C and mixed with Nb powder and loaded in stainless steel targets for the measurement of the $^{10}Be/^{9}Be$ ratios by accelerator mass spectrometry (AMS). AMS measurements were made at the Center for Accelerator Mass Spectrometer at Lawrence Livermore National Laboratory. Details for standards, blanks and age calculations are shown in the footnotes of Table 2.

4.2. Optically stimulated luminescence dating

Samples were collected by hammering opaque plastic tubes, ~20 cm-long, into freshly cleaned natural exposures. The tubes were sealed and placed in light-proof photographic bags until the initial processing at the University of Cincinnati. Laboratory preparation follows the methods described in Seong et al. (2007). The luminescence signals were measured using a Risø TL/OSL reader (model DA-20). Luminescence from the quartz grains was stimulated using an array of blue light-emitting diodes (470 nm, 50 mW/cm^2) filtered using a green long-pass GG-420 filter. Detection was through a Hoya U-340 filter. All quartz aliquots were screened for feldspar contamination using infrared stimulation with infrared light emitting diodes (870 nm, 150 mW/cm^2). All OSL signals were detected using a 52 mm diameter photomultiplier tube (9235B). The equivalent dose (D_e) measurements were determined on multiple aliquots using the single aliquot regenerative (SAR) method protocol developed by Murray and Wintle (2000). Growth curve data were fitted using linear and exponential trend curves. The D_e value for every aliquot was examined using Risø Analysis 3.22b software. Aliquots with poor recuperation (>10%) were not used in the age calculations. Equivalent doses of all aliquots were averaged for each sample then divided by the dose rate giving a mean age (Table 3). Calculation uncertainties and methods used to calculate dose rates are explained in the footnotes in Table 3.

5. Study areas

Detailed studies areas are described from North to South, with the alluvial fan sites listed first (Figs. 1, 2).

5.1. North Ubehebe Crater alluvial fans

A succession of faulted fans is present along the western Grapevine Mountains piedmont near North Ubehebe Crater in northern Death Valley. Frankel and Dolan (2007) first described one of these alluvial fans, which is part of what we informally call the North Ubehebe

Crater alluvial fans, and they used high-resolution LiDAR digital topographic data to quantify the roughness of different age alluvial fan units to aid in regional mapping (Fig. 3). The alluvial fans at this location are composed of a combination of sheet-wash and debris flow deposits, and at least seven alluvial fan units (Q4, Q3c, Q3b, Q3a, Q2c, Q2b and Q2a) can be recognized in this study area (Frankel and Dolan, 2007). Ten quartzite pebbles were collected for TCN dating from the Q2b surface, which has been displaced by the northern Death Valley fault zone. The surface clasts had a mean diameter of 7 cm and ranged from 2 to 13 cm in size.

5.2. Big Dip canyon

Impressive alluvial fans are present at the mouth of Red Wall and Big Dip Canyons radiating from the western flank of the Grapevine Mountains (Fig. 4). Reynolds (1969), Brogan et al. (1991) and Klinger (2001a,b) first examined these alluvial fans. Klinger (2001a,b) mapped six alluvial units, which, based on soil development, he argued ranged in age from late Pleistocene to recent (the active channels), and he documented 250 to 330 m of dextral offset by the northern Death Valley fault zone. The displacement has since been refined to 297 ± 9 m based on LiDAR digital topographic data (Frankel et al., 2007a). Frankel et al. (2007a) used 16 TCN ^{10}Be surface samples and three ^{36}Cl depth profiles to date the Q2c surfaces on the Big Dip Canyon fan to 70 +22/−20 ka and 75 +18/−16 ka, respectively. Approximately 55 ka of ^{36}Cl inheritance was removed from the depth profiles to determine the ^{36}Cl age for this surface. To examine the potential inheritance in active channel cobbles, we collected three cobbles (Sc6A, B and C) from the active channel (Q4b) adjacent to the sampling site for ^{10}Be TCN dating of Frankel et al. (2007a): Fig. 4) at the Big Dip Canyon fan.

5.3. North Junction

Large alluvial fans are also present near North Junction (Figs. 2, 5). Brogan et al. (1991) mapped offsets across a Q3a surface on a fan along the mountain front. A Q3a surface near the mountain front has well preserved channels and is faulted by several strands of the northern Death Valley fault that offset the channels by ~3 m (Fig. 5). We collected quartzite cobbles (DVDFC3A, B, C and D) from the Q3a surface of the alluvial fan and its active channel (Q4b; Sc5A and B) to date using ^{10}Be TCN and to examine any inheritance of TCN.

5.4. South Junction

Small faulted remnants of Q3b alluvial fan surfaces are present at South Junction (Fig. 6). Brogan et al. (1991) first mapped the offsets along these alluvial fans. The Q3b surface and channels are offset several meters by several stands of the northern Death Valley fault. We collected quartzite cobbles (DVDFC2A, C, D and E) from this Q3b surface and its active channel (Q4b; Sc4A, B and C) to date using ^{10}Be TCN and to examine inheritance of TCN.

5.5. Mud Canyon

An impressive succession of alluvial fans is present in the Mud Canyon area. Brogan et al. (1991) mapped offsets along the northern Death Valley fault zone in this region. Frankel et al. (2010a) examined this region in more detail to determine rates of displacement along the northern Death Valley fault zone using airborne LiDAR digital topographic data, ^{10}Be TCN and OSL dating. The OSL dating of Frankel et al. (2010a) shows that the Q3a surface dates to 14–20 ka. However, the ^{10}Be TCN dating could not be used to date the surfaces successfully since the spread of ages is considerable (~38 ka to ~153 ka). Moreover, ^{10}Be TCN in active stream channels shows that inherited TCN concentrations in this area are relatively high, with ages ranging from ~8 to ~30 ka. We examine these data in more detail below and provide new ^{10}Be TCN ages for cobbles from a Q3a surface in the southeastern part of this study area (Fig. 7).

5.6. Beatty Junction bar complex

A series of bars and spits, collectively called the Beatty Junction bar complex by Klinger (2001c), are present north of Beatty Junction. These provide some of the best evidence for Lake Manly and have been examined in numerous studies (Blackwelder, 1933; Hunt and Mabey, 1966; Orme and Orme, 1991; Wright and Troxel, 1993; Galvin and Klinger, 1996; Klinger, 2001a,c). The Betty Junction bar complex comprises four approximately west-trending ridges and spits (A, B, C, and D; Galvin and Klinger, 1996; Klinger, 2001c). The main and highest bar (B) is the youngest and is exposed in a road cut and an excavation just west of the road. The bars and ridges are composed of sand and gravel, which have meter-size beds that mimic the topography of the ridges. The gravels are imbricated, indicating transport direction from the south and west. Galvin and Klinger (1996) hypothesized that the ridges formed in order of increasing crest elevation (from D, C, A, and B).

A case for a Late Pleistocene age as been made for the relative age of the beach ridges based on stratigraphic relationships, preservation of the landforms and soil characteristics (Galvin and Klinger, 1996; Klinger, 2001c). However, the numerical ages for the highest bar are equivocal. Anderson (1998; unpublished data) provides a thermoluminescence (TL) age of 24.0 ± 2.5 ka and an OSL age of ~68 ka for fine-grained sediment ponded behind the main gravel spit near its eastern end (Table 4). The dated sediment was interpreted to have formed in the playa behind the spit, thus these ages post-date the formation of the spit. In contrast, Zreda (cited in Orme an Orme, 1991) and Phillips and Zreda (1999), used ^{36}Cl TCN to date gravel clasts on the spit and for a depth profile through the gravel at the crest of the same spit that give a surface age of 153 ± 13 ka and 20 to 85 ka, respectively.

To test the difference between ages determined on the highest bar (B) we collected two samples for OSL dating from exposures in the bar and quartzite cobbles from the surface of the crest of the bar for ^{10}Be TCN dating (Fig. 8).

5.7. Manly shorelines

A series of wave-cut shorelines are present on the lower slopes of the Black Mountains ~8 km south of Furnace Creek (Figs. 1, 9). The surfaces of these shorelines are armored with small pebbles and cobbles, and desert pavements are present on some stretches. The most prominent wave-cut surface is at an elevation of about 10 m below sea level. We collected cobbles (MANLY-1, -2, -3, -4, -5 and -6) from this surface to help determine the timing of its formation.

6. Dating results

The ^{10}Be TCN and OSL ages for the samples dated in this study are listed in Tables 2 and 3. Table 5 shows the ages from previous studies, which have been calculated using the same methods as described above. All the ^{10}Be TCN ages are minimum ages since we do not make any correction for erosion. Since we have obtained several ^{10}Be TCN ages >350 ka, however, the rate of erosion must be relatively small. Using the method of Lal (1991), the mean erosion rate of the three oldest samples (MANLY-1, KF-0417-12 and -13) was obtained to provide a rough estimate of erosion. This produced values of 5.4 ± 0.6 m/Ma, which are consistent with rates determined in other semi-arid environments (e.g., Small et al., 1997; Seong et al., 2007; Owen et al., 2009) and previous estimates of catchment-scale denudation in

Table 2
Locations for ^{10}Be TCN samples, sample sizes, topographic shielding factors, concentrations, and analytical results and ages.

Sample number and location name	Surface	Lithology	Location		Elevation relative to sea level	Size[a] a/c or a/b/c axes	Thickness	Depth	Production rate atoms/g/yr		Shielding factor	Denudation rate	Quartz[d]	Be carrier[e]	$^{10}Be/^{9}Be$[f]	^{10}Be concentration[f, g, h]	Age[f, i, j]
			Latitude °N	Longitude °W	m	cm	cm	cm	Spallation[b]	Muons[c]		mm/yr	g	mg	x 10^{-13}	10^5 atoms/g SiO_2	ka
North Ubehebe Crater																	
KF-0218-2	Q2b	Quartzite	37.1005	117.4777	844	Cobble	4	0	7.76	0.235	1.0000	0	8.5275	0.3180	6.515 ± 0.166	16.08 ± 0.445	191.1 ± 18.3
KF-0218-3	Q2b	Quartzite	37.1007	117.4791	827	Cobble	4	0	7.66	0.234	1.0000	0	10.0309	0.3290	6.363 ± 0.289	13.81 ± 0.648	164.8 ± 17.0
KF-0218-4	Q2b	Quartzite	37.0958	17.4731	860	Cobble	4	0	7.86	0.236	1.0000	0	10.0141	0.3158	2.269 ± 0.084	4.652 ± 0.183	52.6 ± 5.1
KF-0218-10	Q2b	Quartzite	37.0987	117.4727	855	Cobble	4	0	7.83	0.236	1.0000	0	10.0842	0.3222	2.063 ± 0.075	4.276 ± 0.168	48.6 ± 4.7
KF-0404-1	Q2b	Quartzite	37.0958	117.4721	872	Cobble	4	0	7.93	0.237	1.0000	0	10.0178	0.3093	2.098 ± 0.111	4.199 ± 0.234	47.1 ± 4.9
KF-0404-2	Q2b	Quartzite	37.0959	117.4727	869	Cobble	5	0	7.85	0.236	1.0000	0	10.0524	0.3081	1.242 ± 0.067	2.415 ± 0.140	27.3 ± 2.9
KF-0404-3	Q2b	Quartzite	37.0966	117.4732	864	Cobble	4	0	7.88	0.236	1.0000	0	10.0191	0.3108	1.362 ± 0.661	2.694 ± 1.370	30.2 ± 15.7
KF-0404-4	Q2b	Quartzite	37.0979	117.4738	855	Cobble	5	0	7.76	0.235	1.0000	0	10.0053	0.3075	1.689 ± 0.087	3.339 ± 0.184	38.1 ± 4.0
KF-0404-5	Q2b	Quartzite	37.0989	117.4745	856	Cobble	5	0	7.77	0.235	1.0000	0	10.0009	0.3095	1.976 ± 0.077	3.957 ± 0.164	45.3 ± 4.4
KF-0404-6	Q2b	Quartzite	37.0989	117.4731	863	Cobble	5	0	7.81	0.236	1.0000	0	10.0471	0.3107	1.805 ± 0.070	3.601 ± 0.150	40.9 ± 4.0
Big Dip Canyon																	
Sc6A	Q4b	Chert	36.904	117.293	489	10.9/5.6	8.5	0	5.64	0.208	1.0000	0	21.2134	0.4959	0.320 ± 0.013	0.500 ± 0.020	7.7 ± 0.7
Sc6B	Q4b	Chert	36.904	117.293	489	8.8/5.7	7.5	0	5.69	0.208	1.0000	0	20.5275	0.4993	0.737 ± 0.030	1.199 ± 0.049	18.5 ± 1.8
Sc6C	Q4b	Chert	36.904	117.293	489	14.3/5.8	10	0	5.57	0.208	1.0000	0	22.0755	0.4912	3.170 ± 0.073	4.713 ± 1.086	75.2 ± 6.9
North Junction																	
Sc5A	Q4b	Chert	36.697	117.106	4	12.8/7.2	10	0	3.67	0.177	1.0000	0	21.1193	0.5048	0.573 ± 0.017	0.917 ± 0.027	21.6 ± 2.0
Sc5B	Q4b	Chert	36.697	117.106	4	13.1/6.1	10	0	3.67	0.177	1.0000	0	21.425	0.4962	2.486 ± 0.057	3.853 ± 0.088	92.6 ± 8.5
DVFC3A	Q3a	Chert	36.698	117.105	13	Cobble	5	0	3.77	0.178	0.9777	0	15.1537	0.4488	0.573 ± 0.106	1.137 ± 0.210	26.2 ± 5.4
DVFC3B	Q3a	Chert	36.698	117.105	13	Cobble	5	0	3.86	0.178	1.0000	0	16.2666	0.4443	0.790 ± 0.104	1.444 ± 0.210	32.6 ± 5.2
DVFC3C	Q3a	Chert	36.698	117.105	13	Cobble	5	0	3.86	0.178	1.0000	0	15.2074	0.4306	0.759 ± 0.111	1.438 ± 0.210	32.5 ± 5.6
DVFC3D	Q3a	Chert	36.698	117.105	13	Cobble	5	0	3.86	0.178	1.0000	0	15.2533	0.4477	1.303 ± 0.110	2.559 ± 0.214	58.1 ± 7.1
South Junction																	
Sc4A	Q4b	Chert	36.649	117.034	85	10.7/5.6	8.5	0	4	0.182	1.0000	0	20.451	0.4984	0.167 ± 0.012	0.273 ± 0.019	5.9 ± 0.7
Sc4B	Q4b	Chert	36.649	117.034	85	12.3/5.9	9.5	0	3.97	0.182	1.0000	0	20.6892	0.4993	0.193 ± 0.016	0.312 ± 0.026	6.8 ± 0.8
Sc4C	Q4b	Chert	36.649	117.034	85	11.1/6.8	9	0	3.99	0.182	1.0000	0	24.1426	0.4984	2.057 ± 0.047	2.841 ± 0.066	62.6 ± 5.7
DVFC2A	Q3b	Chert	36.650	117.035	90	Cobble	5	0	3.95	0.183	0.9554	0	16.2013	0.4780	0.145 ± 0.104	0.286 ± 0.206	6.3 ± 4.5
DVFC2C	Q3b	Chert	36.650	117.035	90	Cobble	5	0	3.92	0.183	0.9474	0	8.0543	0.4053	0.132 ± 0.102	0.452 ± 0.345	9.8 ± 7.7
DVFC2D	Q3b	Chert	36.650	117.035	90	Cobble	5	0	3.92	0.183	0.9474	0	8.4554	0.4401	0.087 ± 0.101	0.302 ± 0.353	6.7 ± 7.8[k]
DVFC2E	Q3b	Chert	36.650	117.035	90	Cobble	5	0	4.14	0.183	1.0000	0	15.1772	0.4381	1.393 ± 0.110	2.692 ± 0.212	57.1 ± 6.8

Mud Canyon																	
KF-0416-1	Q3a	Quartzite	36.6196	116.9390	18	Cobble	4	0	3.91	0.179	1.0000	0	30.0419	0.4840	1.385 ± 0.045	1.160 ± 0.053	25.8 ± 2.5
KF-0416-2	Q3a	Quartzite	36.6196	116.9939	18	Cobble	4	0	3.91	0.179	1.0000	0	30.2397	0.4682	0.647 ± 0.039	0.341 ± 0.043	7.6 ± 1.2
KF-0416-3	Q3a	Quartzite	36.6197	116.9939	20	Cobble	5	0	3.88	0.179	1.0000	0	30.0195	0.4683	2.973 ± 0.084	2.767 ± 0.094	62.6 ± 5.9
KF-0416-4	Q3a	Quartzite	36.6192	116.9939	20	Cobble	5	0	3.88	0.179	1.0000	0	30.0587	0.4887	0.957 ± 0.038	0.708 ± 0.045	15.8 ± 1.7
KF-0416-5	Q3a	Quartzite	36.6199	116.9937	18	Cobble	5	0	3.88	0.178	1.0000	0	30.101	0.4931	5.602 ± 0.138	5.800 ± 0.164	133.8 ± 12.6
KF-0416-6	Q3a	Quartzite	36.6201	116.9935	21	Cobble	5	0	3.88	0.179	1.0000	0	30.4084	0.4932	1.052 ± 0.034	0.813 ± 0.041	18.2 ± 1.8
Beatty Junction bar complex																	
KF041710	Lake Manly shorelines	Chert	36.620	116.994	45	Cobble	4	0	3.97	0.18	1.0000	0	20.0139	0.4927	3.294 ± 0.084	5.425 ± 0.139	121.9 ± 11.4
KF041711	Lake Manly shorelines	Chert	36.620	116.994	45	Cobble	4	0	3.96	0.18	1.0000	0	20.1133	0.4729	4.640 ± 0.179	7.300 ± 0.282	166.1 ± 16.5
KF041712	Lake Manly shorelines	Chert	36.620	116.994	45	Cobble	2	0	4.03	0.18	1.0000	0	20.1282	0.5037	9.717 ± 0.029	16.27 ± 0.487	384.8 ± 39.1
KF041713	Lake Manly shorelines	Chert	36.619	116.994	45	Cobble	3	0	4	0.18	1.0000	0	20.0566	0.4839	9.668 ± 0.231	15.61 ± 0.373	370.2 ± 36.7
KF041714	Lake Manly shorelines	Chert	36.620	116.994	45	Cobble	4	0	3.96	0.18	1.0000	0	20.0913	0.5022	3.175 ± 0.081	5.310 ± 0.136	119.4 ± 11.2
KF041715	Lake Manly shorelines	Chert	36.620	116.994	45	Cobble	5	0	3.93	0.179	1.0000	0	20.0184	0.4852	3.909 ± 0.097	6.340 ± 0.157	144.7 ± 13.6
Lake Manly shorelines (~8 km south of Furnace Creek)																	
MANLY-1	Lake Manly shorelines	Quartzite	36.3844	116.8461	−10	12/10/5	5	0	3.77	0.177	1.0000	0	30.1921	0.3705	19.96 ± 0.386	16.34 ± 0.357	465.4 ± 47.0
MANLY-2	Lake Manly shorelines	Quartzite	36.3844	116.8461	−10	9/9/4.0	4	0	3.8	0.177	1.0000	0	30.9697	0.3488	6.668 ± 0.158	4.997 ± 0.129	130.0 ± 12.2
MANLY-3	Lake Manly shorelines	Quartzite	36.3844	116.8461	−10	11/8/6.0	6	0	3.74	0.177	1.0000	0	30.036	0.3466	6.958 ± 0.133	5.343 ± 0.115	141.5 ± 13.1
MANLY-4	Lake Manly shorelines	Quartzite	36.3844	116.8461	−10	11/8/6.0	6	0	3.74	0.177	1.0000	0	30.5161	0.3729	13.02 ± 0.274	10.61 ± 0.248	291.9 ± 28.3
MANLY-5	Lake Manly shorelines	Quartzite	36.3844	116.8461	−10	8/7/5.0	5	0	3.77	0.177	1.0000	0	30.3504	0.4075	5.089 ± 0.097	4.543 ± 0.098	118.7 ± 11.0
MANLY-6	Lake Manly shorelines	Quartzite	36.3844	116.8461	−10	13/10/9.0	5	0	3.77	0.177	1.0000	0	30.1771	0.3965	4.800 ± 0.916	4.192 ± 0.091	109.3 ± 10.1

[a] Cobbles ~10 cm in diameter.

[b] Constant (time-invariant) local production rate based on Lal (1991) and Stone (2000). A sea level, high-latitude value of 4.5 ± 0.3 at ^{10}Be g^{-1} quartz was used.

[c] Constant (time-invariant) local production rate based on Heisinger et al. (2002a,b).

[d] A density of 2.7 g cm^{-3} was used for all surface samples.

[e] Concentration of carrier for all Sc samples was 1410 ppm, all DVFC samples was 437 ppm and all other samples was 1000 ppm.

[f] Isotope ratios were normalized to ^{10}Be standards prepared by Nishiizumi et al. (2007) with a value of 2.85×10^{-12} and using a ^{10}Be half life of 1.36×10^{6} years. Uncertainties are reported at the 1σ confidence level.

[g] Samples beginning with Sc4, Sc5, Sc6, and DVFC were corrected for a mean blank $^{10}\text{Be}/^{9}\text{Be} = 1.99 \pm 0.48 \times 10^{-15}$, samples beginning with KF were corrected for a mean blank $^{10}\text{Be}/^{9}\text{Be} = 6.183 \pm 0.833 \times 10^{-15}$, and samples beginning with MANLY were corrected for a mean blank $^{10}\text{Be}/^{9}\text{Be} = 3.028 \pm 0.353 \times 10^{-15}$.

[h] Propagated uncertainities include error in the blank, carrier mass (1%), and counting statistics.

[i] Propagated error in the model ages include a 6% uncertainty in the production rate of ^{10}Be and a 4% uncertainty in the ^{10}Be decay constant.

[j] Beryllium-10 model ages were calculated with the CRONUS-Earth online calculator, version 2.2 (Balco et al., 2008; http://hess.ess.washington.edu/).

[k] The large error is a reflection of the large AMS measurement uncertainty.

Table 3
Summary of OSL dating results from extracted from sediment, sample locations, radioisotopes concentrations, moisture contents, total dose-rates, D_e estimates and optical ages.

Laboratory number	Location (°N/°W)	Altitude (m asl)	Depth (cm)	Particle Size (μm)	U[a] (ppm)	Th[a] (ppm)	K[a] (%)	Rb[a] (ppm)	Cosmic[b, c] (G/ka)	Dose-rate[b, d] (G/ka)	n[e]	Mean equivalent dose[f] (Gy)	OSL Age[h,i] (ka)
KF11	36.613/116.946	45	90	180–250	3.70	9.05	1.80	70.5	0.19 ± 0.02	2.96 ± 0.18	32 (36)	54.8 ± 1.6	18.3 ± 1.2
KF12	36.613/116.946	45	90	180–250	3.34	9.73	1.95	76.0	0.19 ± 0.02	3.05 ± 0.19	33 (36)	59.3 ± 1.6	19.4 ± 1.3

[a]Elemental concentrations from NAA of whole sediment measured at USGS Nuclear Reactor Facility in Denver (Budahn and Wandless, 2002). Uncertainty taken as ± 10%.
[b]Estimated fractional present-day water content for whole sediment is taken as 10 ± 5%.
[c]Estimated contribution to dose-rate from cosmic rays calculated according to Prescott and Hutton (1988). Uncertainty taken as ± 10%.
[d]Total dose-rate from beta, gamma and cosmic components. Beta attenuation factors for U, Th and K compositions incorporating grain size factors from Mejdahl (1979). Beta attenuation factor for Rb is taken as 0.75 (cf. Adamiec and Aitken, 1998). Factors utilized to convert elemental concentrations to beta and gamma dose-rates from Adamiec and Aitken (1998) and beta and gamma components attenuated for moisture content.
[e]Number of replicated equivalent dose (D_e) estimates used to calculate weighted mean D_e. These are based on recuperation error of < 10%. The number in the parenthesis is the total measurements made including failed runs with unusable data.
[f]Weighted mean equivalent dose (D_e) determined from replicated single-aliquot regenerative-dose (SAR; Murray and Wintle, 2000) runs. The uncertainty also includes an error from beta source estimated of ± 5%.
[h]Uncertainty incorporate all random and systematic errors, including dose rates errors and uncertainty for the $D_{e.}$
[i]Weighted mean of two dose rates from two sets of NAA were used to determine the age.

Death Valley and neighboring Panamint Valley (Jayko, 2005). If we assume that all the samples we collected erode at that rate, then a calculated age of 10 ka would underestimate the true age by ~5%, an age of 50 ka by ~24%, and an age of 100 ka by ~50%. However, since most of the clasts (cobbles and boulders) we collected retained their original rounded depositional shapes, and given the arid to semi-arid climate in the region throughout the late Quaternary, it is highly unlikely that these clasts have experienced any significant erosion.

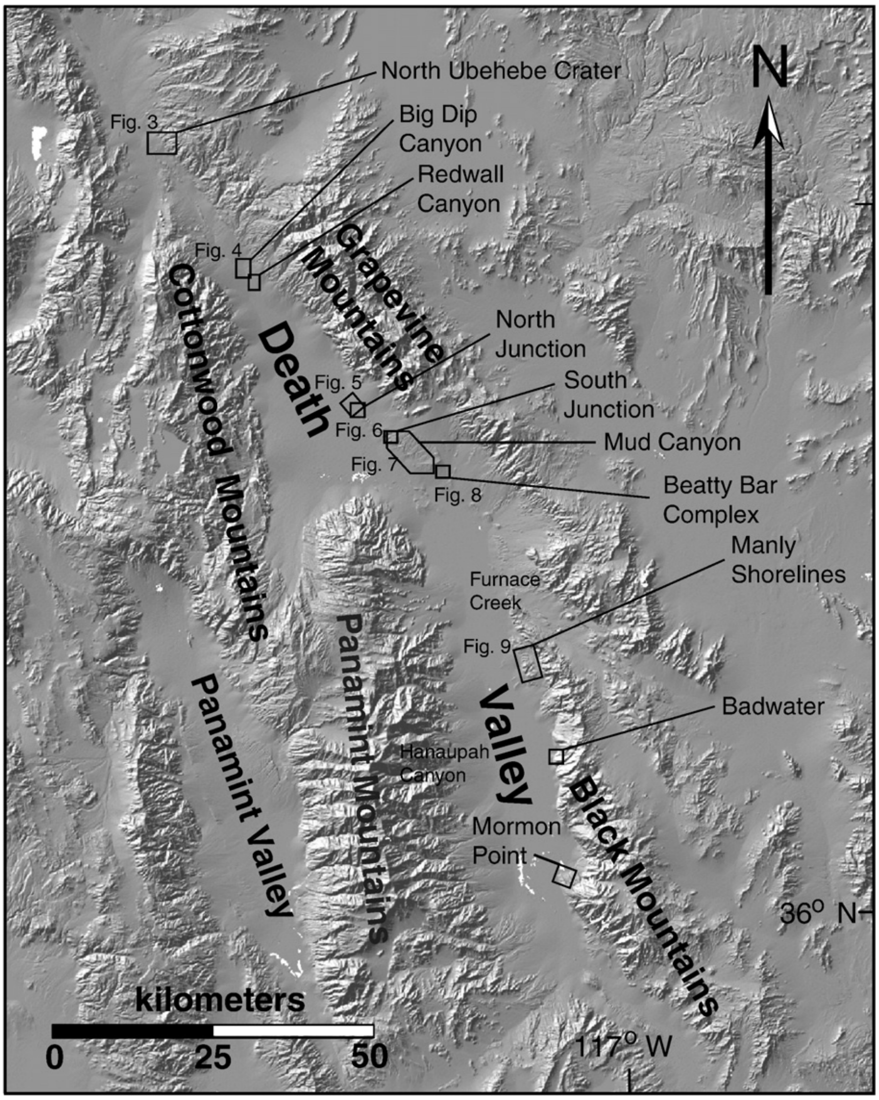

Fig. 2. Map of Death Valley showing the locations of Quaternary surfaces that have been dated using numerical methods and the study areas examined in this paper.

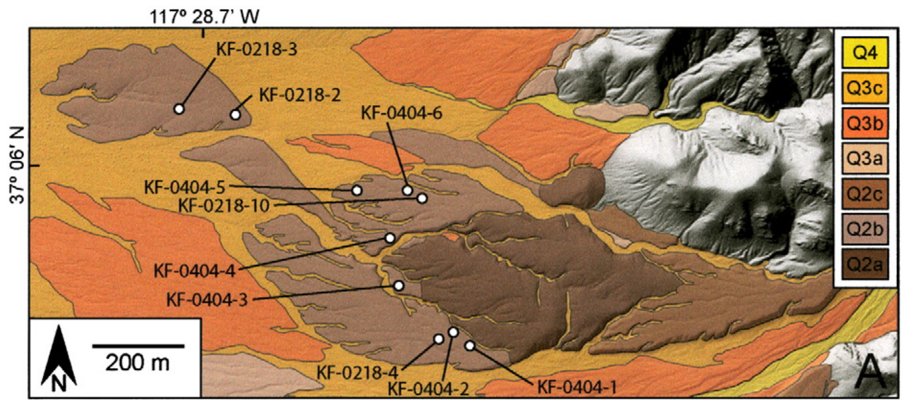

Fig. 3. High-resolution airborne LiDAR digital topographic image for the North Ubehebe Crater study area (adapted from Frankel and Dolan, 2007) showing locations for the ^{10}Be TCN sampling.

Currently, there is much debate regarding the appropriate scaling models and geomagnetic corrections for TCN production to calculate TCN ages (e.g., Pigati and Lifton, 2004; Staiger et al., 2007; Balco et al., 2008). We therefore use constant (time-invariant) local production based on Lal (1991) and Stone (2000), but acknowledge that uncertainties in absolute production rates for the latitude and

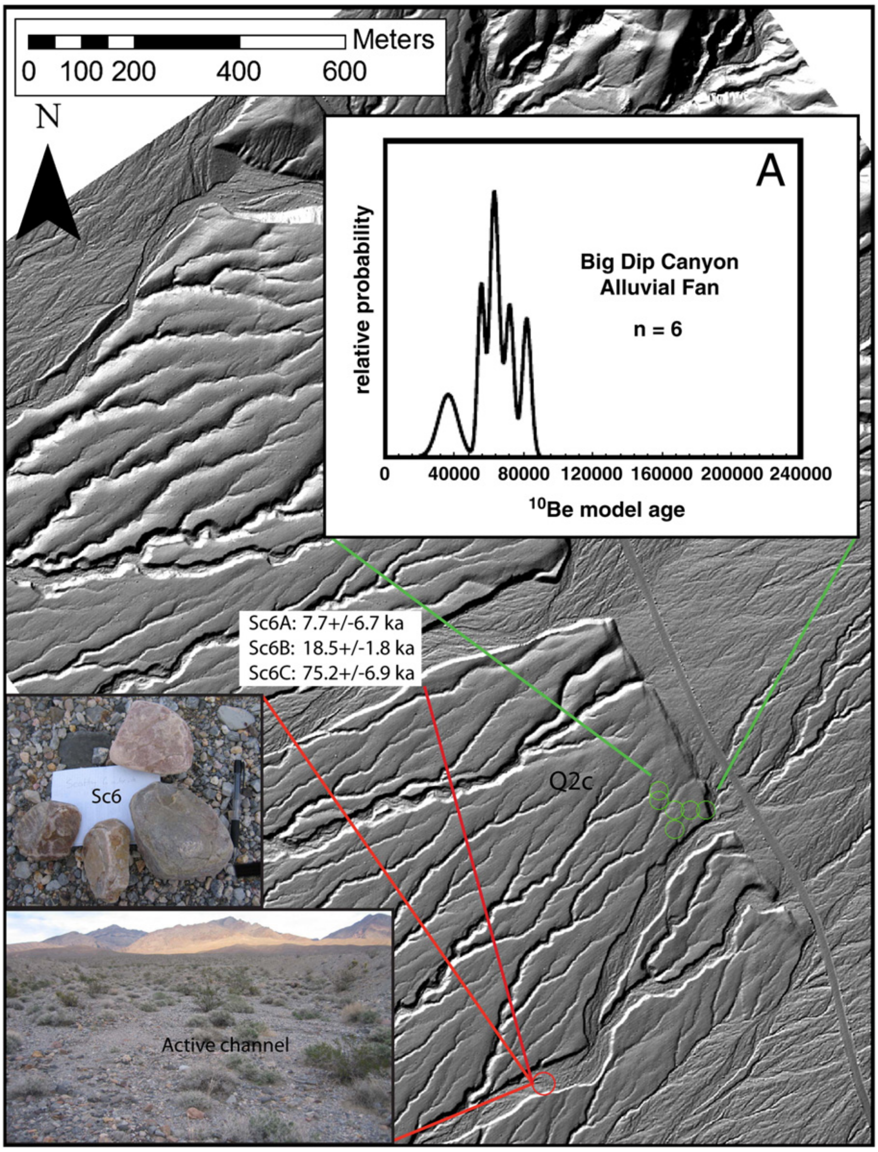

Fig. 4. High-resolution airborne LiDAR digital topographic image for Big Dip Canyon showing the locations of sampling sites for ^{10}Be TCN dating. The green circles show the sites sampled by Frankel et al. (2007a) together with a probability distribution plot for their ages. The red circles show the locations of the samples (Sc6A, B, C) sampled from the active channel together with photographs of the active channel and typical sampled clasts.

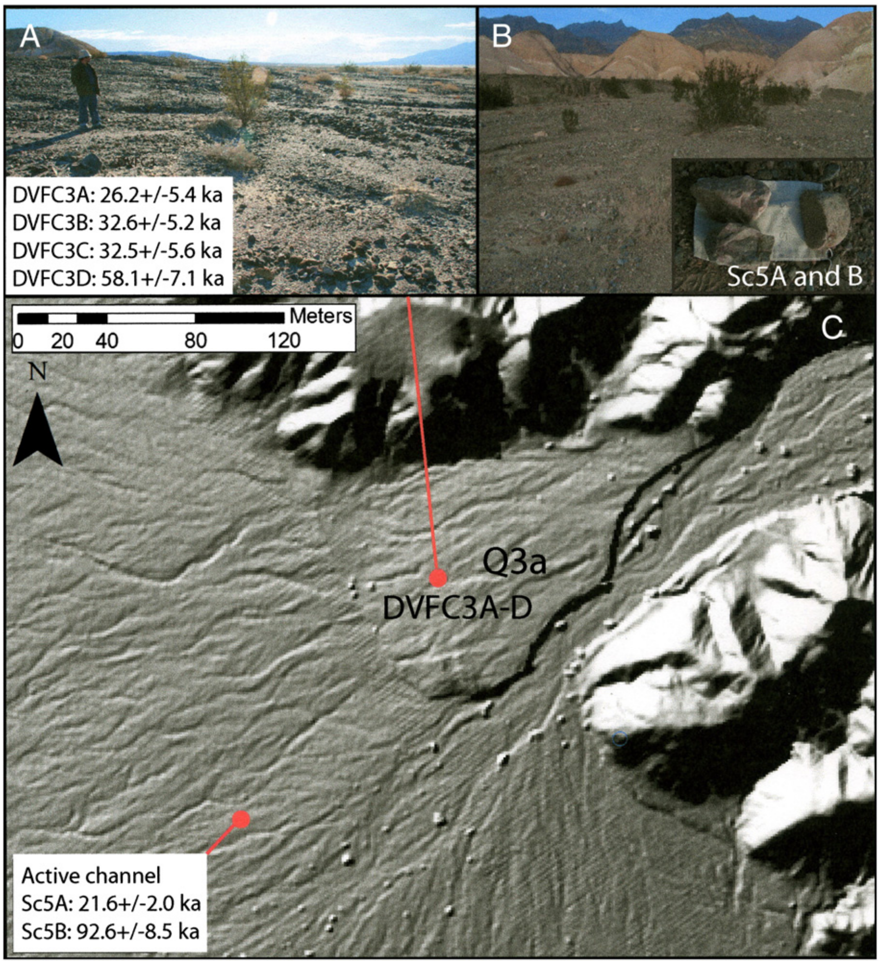

Fig. 5. Dating sites at the North Junction alluvial fans. A) View of the Q3a fan together with ^{10}Be TCN ages. B) View of active channel with examples of the typical clasts that were dated using ^{10}Be TCN methods. C) High-resolution airborne LiDAR digital topographic image of the sampled areas.

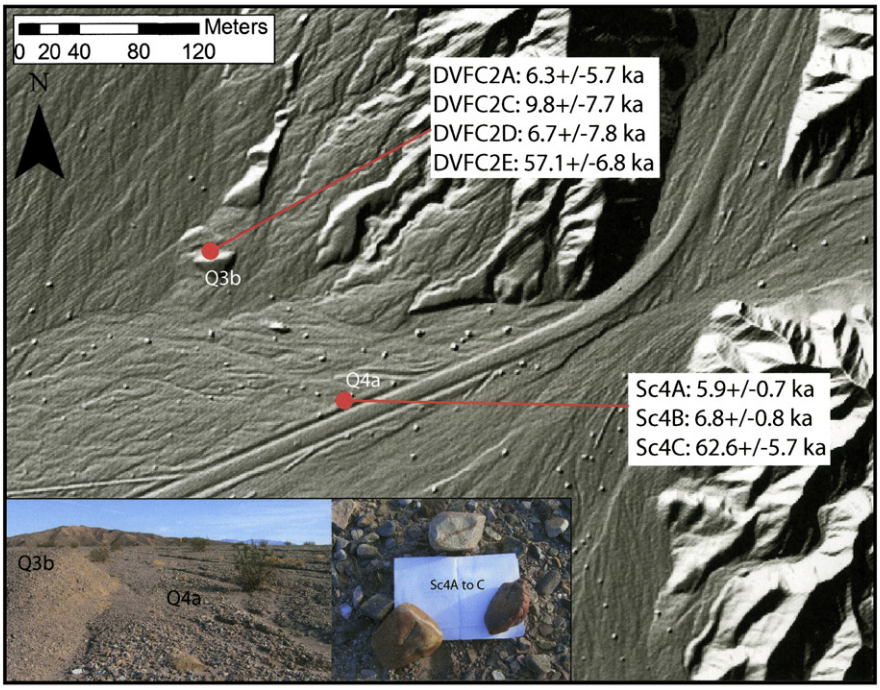

Fig. 6. High-resolution airborne LiDAR digital topographic image of the South Junction study area showing the location of the sampling sites and views of the Q3b surface, and the active channel with typical clasts that were sampled for ^{10}Be TCN dating.

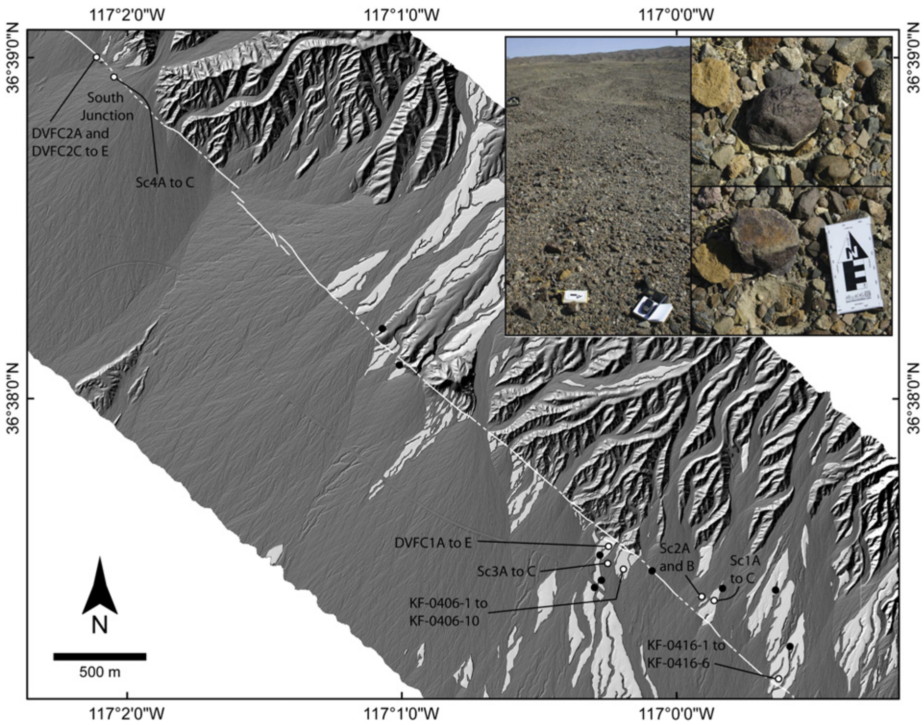

Fig. 7. High-resolution airborne LiDAR digital topographic image for South Junction and Mud Canyon (adapted from Frankel et al., 2010a) showing the sampling locations for ^{10}Be TCN (white circles) and the OSL dating sites (black circles) of Frankel et al. (2010a). Q3a surfaces are shaded in pale grey. The white lines show the trace of the dextral northern Death Valley fault. The inset photographs show a typical surface for Q3a where samples KF-0416-1 to KF-0416-6 where sampled and an example of one of the sampled clast, showing both the exposed and underside surface (lower panel).

altitudes of Death Valley may be up to ≤15% different in apparent age among scaling models for the Holocene and ≤10% for the late Pleistocene. Irrespective of these issues, scaling factors have far less impact on relative chronologies for events in a limited geographic area, such as our study area in Death Valley.

All of our ^{10}Be TCN ages show considerable variance on individual surfaces (Tables 2, 5). For example, the Q2b surface in the North Ubehebe Crater study area has ^{10}Be TCN ages that range from ~27 ka to ~191 ka, the Q3a surface in Mud Canyon has ages that range from ~8 to ~133 ka, the Q3a surface at North Junction has ages that range from ~26 ka to ~51 ka, and the Q3b surface at South Junction has ages from ~6 ka to ~134 ka. Moreover, samples collected in the active channels (Q4a) range from ~6 ka to ~93 ka. Similarly, the spread of ^{10}Be TCN ages for the Beatty Junction bar complex and the Manly shorelines study area is large, ranging from ~119 ka to ~385 ka (mean = 218 ka; 1 σ[standard deviation] = 125 ka) and ~109 ka to ~465 ka (mean = 209 ka; 1 σ = 142 ka), respectively. There is no correlation between sample size (boulder/cobble) and age within an individual surface (Tables 2, 5) or with source area size or transport distance to depocenter. To fully assess the spread of ^{10}Be TCN ages on the alluvial fan surfaces, we plot all the ^{10}Be TCN ages determined in this and previous studies for Death Valley as probability distributions (Fig. 10).

Both OSL samples have ages that are within error of each other showing that the sands were deposited at ~19 ka. This provides confidence in the OSL dating.

7. Discussion

TCN ages on surfaces are affected by several geological factors, including weathering, exhumation, prior exposure, and shielding of the surface by sediment and/or snow. With the exception of prior exposure, these factors generally reduce the concentration of TCNs in surfaces, which results in an underestimate of the true age of the landforms. Episodes of prior exposure result in an overestimate of the true age. Uneven distribution of these geological processes can produce a large spread in apparent exposure ages on a landform. These effects are commonly assessed by collecting multiple samples on a surface. If multiple surface samples possess similar apparent ages, the data suggest that the dated samples were not derived from older surfaces and/or were not weathered or exhumed; hence the ages are

Table 4
Numerical ages from the highest spit of the Betty Junction bar complex (adapted from Machette et al., 2001).

Location	Reference	Elevation (m asl)	Analytical technique	Age (ka)
Back bar, eastern end	Anderson, 1998	45	TL	24.5 ± 2.5 (min.)
		45	OSL	~68 (min.)
Crest of spit in road cut	Phillips and Zreda, 1999	46	^{36}Cl (gravel in profile)	20–85 (minimum–maximum)
Crest of spit	Zreda, 1991, cited in Orme and Orme, 1991	46	^{36}Cl (gravel on surface)	153 ± 13
Crest of spit in road cut	This study	45	OSL	18.9 ± 1.3
Crest of spit	This study	46	^{10}Be	119–385

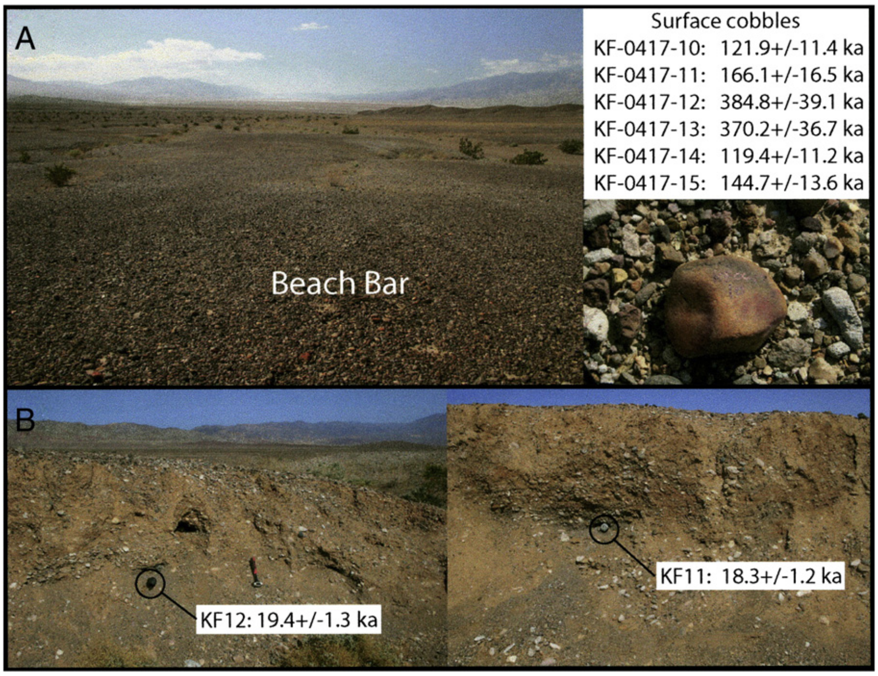

Fig. 8. The highest bar (B) of the Beatty Junction bar complex showing A) the surface and example of the cobbles that were dated together with ^{10}Be TCN ages and B) sampling locations for OSL dating in excavations.

probably representative of the "true" age of the surface. In the typical case where a wide range of the ages are obtained for a single landform, the most likely explanation suggests post-depositional exhumation of fresh boulders to the surface and/or derivation of samples from deposits or slopes that have experienced prior exposure to cosmic rays, thus containing inherited TCN concentrations. The large spread of ages on individual surfaces in Death Valley reflects the dominance of geologic processes in controlling the concentrations of TCNs in clasts and sediment.

The very large spread of ages for the cobbles and boulders in the active channels (Q4a surfaces) clearly indicates that the ^{10}Be TCN concentrations in the sampled clasts have a significant inherited component (Fig. 10A). The minimum age for any clast in this and Frankel et al.'s (2007a, 2010a,b) studies is 2 ka, but the mean is 24 ka and standard deviation is 27 ka (strongly skewed toward younger ages). This suggests that clasts within older alluvial fan surfaces will have a significant component of inherited ^{10}Be TCNs.

Table 6 shows the ^{10}Be TCN ages for alluvial fan surfaces that were dated in this study and in Frankel et al. (2007a; 2010a,b). These are compared with the age estimates of Klinger (2001a,b,d), which were based on soil characteristics, and the OSL ages of Sohn et al. (2007) and Frankel et al. (2010a,b). These data show that the mean ^{10}Be TCN ages of Q3a, Q3b and Q3c surfaces are considerably older than the estimated ages of the surfaces based on OSL and soil methods (Fig. 10B). However, the youngest ^{10}Be TCN ages for each surface are consistent with the estimated ages, which indicate that the sampled clasts probably have significant inherited TCNs. The prevalence of inherited ^{10}Be TCNs in samples suggests that sediment transfer to alluvial fans from adjacent hillslopes is slow.

Death Valley is dominated (almost exclusively) by bedrock hillslopes, for which very little is understood in terms of geomorphic transport laws compared with soil mantled landscapes (e.g., Howard and Selby, 1994; Perron et al., 2009). The inheritance in the TCN data may suggest that these bedrock landscapes behave in a manner consistent with stochastic mass movements. By and large, though, material appears to remain on hillslopes, exposed to cosmic rays, for long periods of time (10^3–10^5 years) and may also experience considerable residence time (many millennia to tens of millennia) on valley sides (floodplains) or in catchment bottoms following transport from hillslope to channel.

These results highlight the problems of applying TCN methods to surface samples to date alluvial fans in Death Valley. Machette et al. (2008) showed that the use of TCN depth profiles might help assess and overcome the problems of inheritance. Moreover, Frankel et al. (2007a) showed that both surface clasts and depth profiles could be used to define ages with confidence in some settings. However, Frankel et al. (2010b) showed that depth profiles could not be determined on Q3 surfaces because the amount of TCN inheritance in sediment is several orders of magnitude greater than the concentrations of TCN acquired *in situ*.

The distribution of ^{10}Be TCN ages for Q2c has a similarly large range, but the younger ^{10}Be TCN ages are close to the age estimate of the surfaces based on other methods (Fig. 10C). The spread of ^{10}Be TCN ages for Q2b, based on only one study area (North Ubehebe Crater), is also large but the youngest ages are significantly younger than age estimates based on other relative weathering and soil methods. This suggests that erosion may be significant on these surfaces, exhuming clasts and exposing them late in the evolutionary history of the fan. Inheritance may also be a problem for some clasts on the Q2b surfaces, as highlighted by the samples (KF-0218-2 and -3) which are older than 160 ka. The Q2b surface age would be 41 ± 9 ka if the two oldest samples were eliminated from the dataset. This would be a significant reduction of the age, and thus argues for significant erosion of this surface. The surface erosion interpretation suggested by the TCN ages is supported by abundant incised channels that traverse Q2b and the development of a convex hillslope-type system on alluvial fans of this age in the North Ubehebe Crater area, thus providing geomorphic evidence for extensive erosion of this fan (Fig. 3; e.g, Frankel and Dolan, 2007).

The large spread of ^{10}Be TCN ages for the Beatty Junction bar complex (~119 ka to ~385 ka; mean = 218 ka; σ = 125 ka) and the Manly shorelines (~109 ka to ~465 ka; mean = 209 ka; σ = 142 ka)

Table 5
Location and ^{10}Be TCN ages for samples collected from fan surfaces in the Mud Canyon region (from Frankel et al., 2010a), Badwater and Mormon Point (after Frankel et al., 2010b), and Red Wall Canyon and Big Dip Canyon (after Frankel et al., 2007a). All ages were calculated or recalculated using the same methods as in our study.

Sample name and location	Surface	Location		Elevation	Size a/b axes	Age
		Latitude	Longitude			
		°N	°W	m asl	cm	ka
Mud Canyon						
Sc2A	Q4b	36.624	116.998	38	Cobble: 9.2/5.9	12.7 ± 1.3
Sc2B	Q4b	36.624	116.998	38	Cobble:12.7/6.5	27.3 ± 2.7
Sc3A	Q4b	36.625	117.004	31	Cobble: 10.5/9.1	9.8 ± 0.9
Sc3B	Q4b	36.625	117.004	31	Cobble: 9.1/5.4	30.2 ± 2.7
Sc3C	Q4b	36.625	117.004	31	Cobble: 11.7/7.2	7.9 ± 0.8
Sc1A	Q3a	36.624	116.998	46	Cobble: 13/6.8	68.7 ± 6.3
Sc1B	Q3a	36.624	116.998	46	Cobble: 14.2/5.1	49.0 ± 4.5
Sc1C	Q3a	36.624	116.998	46	Cobble: 13.8/4.2	50.5 ± 4.6
DVFC1A	Q3a	36.626	117.004	57	Cobble: ~10 cm	152.6 ± 15.1
DVFC1B	Q3a	36.626	117.004	57	Cobble: ~10 cm	78.4 ± 8.3
DVFC1C	Q3a	36.626	117.004	57	Cobble: ~10 cm	81.0 ± 8.7
DVFC1D	Q3a	36.626	117.004	57	Cobble: ~10 cm	82.4 ± 9.0
DVFC1E	Q3a	36.626	117.004	57	Cobble: ~10 cm	80.1 ± 8.8
KF-0406-1	Q3a	36.6255	117.0032	44	Cobble: ~10 cm	63.2 ± 6.0
KF-0406-2	Q3a	36.6253	117.0032	41	Cobble: ~10 cm	77.8 ± 7.3
KF-0406-3	Q3a	36.6253	117.0033	38	Cobble: ~10 cm	69.9 ± 6.6
KF-0406-4	Q3a	36.6254	117.0036	40	Cobble: ~10 cm	37.7 ± 3.7
KF-0406-5	Q3a	36.6252	117.0034	31	Cobble: ~10 cm	76.0 ± 7.1
KF-0406-6	Q3a	36.6251	117.0029	33	Cobble: ~10 cm	57.3 ± 5.4
KF-0406-7	Q3a	36.6253	117.0032	38	Cobble: ~10 cm	99.9 ± 9.9
KF-0406-8	Q3a	36.6251	117.0031	34	Cobble: ~10 cm	58.4 ± 5.5
KF-0406-9	Q3a	36.6251	117.0033	35	Cobble: ~10 cm	78.2 ± 7.0
KF-0406-10	Q3a	36.6250	117.0037	32	Cobble: ~10 cm	122.1 ± 11.5
Faulted fans south of Badwater						
Bwater6	Q4b	36.2250	116.7707	−10	Sediment <2	18.2 ± 1.9
Bwater7	Q4b	36.2250	116.7706	−13	Cobble: 8.0/8.0/5.0	18.6 ± 1.7
Bwater8	Q4b	36.2250	116.7706	−9	Cobble: 15.0/11.0/3.0	4.0 ± 0.5
BWF081	Q4b	36.2255	116.7714	−17	Boulder: 100/50/25	73.4 ± 6.7
BWF082	Q4b	36.2253	116.7715	−14	Boulder: 160/90/70	10.8 ± 1.1
BWF083	Q4b	36.2257	116.7712	−19	Boulder: 80/60/60	3.7 ± 0.7
BWF084	Q4b	36.2257	116.7712	−20	Boulder: 125/110/60	3.2 ± 0.4
BWF085	Q4b	36.2261	116.7713	−25	Boulder: 160/130/65	2.0 ± 0.5
Bwater1	Q3c	36.2260	116.7711	−19	Cobble: 16.5/11.5/9.5	10.2 ± 1.1
Bwater2	Q3c	36.2261	116.7711	−19	Cobble: 16.5/10.5/7.5	17.6 ± 1.8
Bwater3	Q3c	36.2261	116.7711	−19	Cobble: 21.5/13.5/10.5	9.6 ± 0.9
Bwater4	Q3c	36.2262	116.7711	−21	Cobble: 12.5/7.5/4.5	43.2 ± 3.9
Bwater5	Q3c	36.2262	116.7712	−24	Cobble: 12.0/9.0/7.0	16.9 ± 1.7
Small fan east of Badwater						
BWF086	Q3c	36.2328	116.7630	−19	Boulder: 140/90/60	14.2 ± 1.4
BWF088	Q3c	36.2328	116.7631	−18	Boulder: 135/130/60	1.8 ± 0.4
BWF089	Q3c	36.2328	116.7631	−22	Boulder: 110/80/90	5.8 ± 0.9
Mormon Point						
KFMP101	Q3b	36.0618	116.7564	−49	Cobble: ~10 cm	49.4 ± 4.8
KFMP103	Q3b	36.0618	116.7564	−49	Cobble: ~10 cm	15.7 ± 1.5
KFMP105	Q3b	36.0618	116.7564	−49	Boulder: ~50 cm	4.0 ± 0.5
KFMP106	Q3b	36.0618	116.7564	−49	Cobble: ~10 cm	10.4 ± 1.0
KFMP110	Q3b	36.0618	116.7564	−49	Cobble: ~10 cm	9.6 ± 1.0
KFMP112	Q3b	36.0618	116.7564	−49	Cobble: ~10 cm	14.1 ± 1.4
Red Wall Canyon						
KF-031605-1	Q2c	36.8700	117.2600	401	Cobble: ~20 cm	235.5 ± 22.1
KF-031605-2	Q2c	36.8763	117.2625	393	Cobble: ~20 cm	81.4 ± 7.5
KF-031605-3	Q2c	36.8755	117.2605	391	Cobble: ~20 cm	134.1 ± 12.4
KF-031605-4	Q2c	36.8762	117.2598	398	Cobble: ~20 cm	65.6 ± 6.3
KF-031605-5	Q2c	36.8758	117.2585	399	Cobble: ~20 cm	73.7 ± 6.8
KF-031605-7	Q2c	36.8738	117.2592	377	Cobble: ~20 cm	69.8 ± 6.8
KF-031605-8	Q2c	36.8728	117.2583	372	Cobble: ~20 cm	76.3 ± 7.3
KF-031605-9	Q2c	36.8722	117.2560	371	Cobble: ~20 cm	93.0 ± 8.7
KF-031605-10	Q2c	36.8712	117.2557	361	Cobble: ~20 cm	75.9 ± 7.1
KF-RWC-03	Q2c	36.8700	117.2533	355	Cobble: ~20 cm	75.8 ± 7.1
Big Dip Canyon						
Q2C1	Q2c	36.9082	117.2898	500	Cobble: ~10 cm	81.9 ± 7.7
Q2C2	Q2c	36.9083	117.2898	500	Cobble: ~10 cm	63.3 ± 6.0
Q2C3	Q2c	36.9080	117.2895	500	Cobble: ~10 cm	92.8 ± 8.8
Q2C4	Q2c	36.9080	117.2892	500	Cobble: ~10 cm	73.5 ± 7.1
Q2C5	Q2c	36.9077	117.2895	500	Cobble: ~10 cm	70.5 ± 6.7
Q2C6	Q2c	36.9080	117.2888	500	Cobble: ~10 cm	41.3 ± 7.3

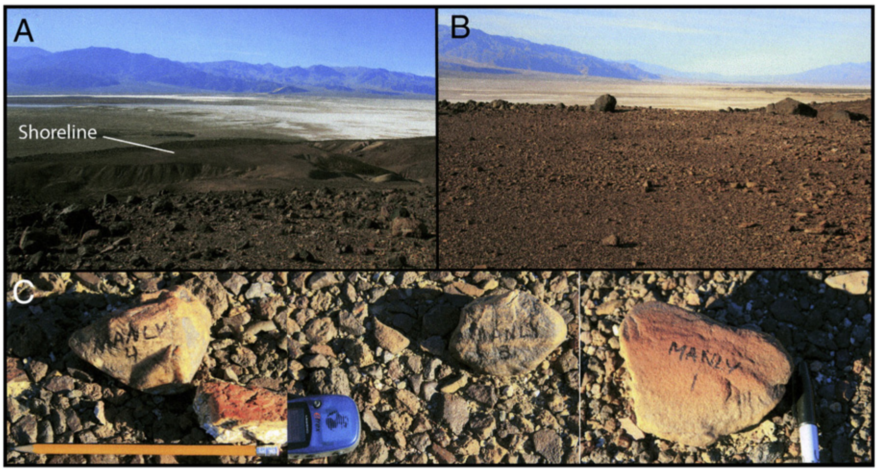

Fig. 9. Views of Manly shorelines ~8 km south of Furnace Creek. A) View NW across Death Valley showing the location of the shoreline from where ^{10}Be TCN samples were collected. B) Surface of the shoreline that was samples. C) Views of several of the sampled cobbles on surface of the shoreline.

study areas also suggests that geologic factors have a strong influence on these surfaces. The OSL dates (Table 3) for the Beatty Junction bar complex are similar to the TL date of Anderson (1998; unpublished data), but are significantly different than the OSL date of Anderson (1998) (Table 4). Moreover, the soil development characteristics are consistent with a late Pleistocene age (Galvin and Klinger, 1996; Klinger, 2001c); however, correlating soil development on alluvial-fan deposits with soils developed on a gravel spit is equivocal. Li et al. (1996) and Lowenstein et al. (1999) interpreted sediment cores from near Badwater as consistent with a "deep" Lake Manly during marine isotope stage (MIS) 2 and towards the end of MIS 6. However, core recovery of MIS 2 sediments was poor and the faunal data are consistent with a saline mudflat rather than a freshwater lake (Forester et al., 2005). In addition, Machette et al. (2008) and Knott et al. (2002, 2004) found no evidence of an MIS 2 lake above −46 m and −30 m, respectively, on morphologically similar alluvial-fan deposits dated to between 100 and 40 ka by Machette et al. (2008). Finally, Matsubara and Howard (2009) found that climate models do not support a "deep" Lake Manly at MIS 2 along with deep Lake Lahonton and Lake Bonneville.

The disparate geochronology at the Beatty Junction bar complex leads to two possible interpretations of the TCN data. If the Beatty bar was deposited during MIS 2, then the OSL dates (Table 3), TL dates of Anderson (1998) and soil development represent the correct age of the deposit at the Beatty bar. This would represent a high lake-level stand during MIS 2 at +45 m (~130 m deep lake) and that the TCN-dated cobbles have ~170 ka inherited ^{10}Be. This interpretation is consistent with the interpretation of core data by Lowenstein et al. (1999).

Alternatively, if the Beatty bar was deposited during MIS 6, then the TCN ^{10}Be-dated cobbles have ~20 ka inherited ^{10}Be and the OSL dates (Table 3) and the soil development reflects material washed into the bar deposit long after deposition. The washed-in materials would have been bleached (reset) and will therefore record younger dates. This interpretation is consistent with observations by Machette et al. (2008) and Knott et al. (2002, 2004) that no lacustrine deposition or erosion is observed on 100–40 ka alluvial-fan deposits at Hanaupah Fan and Mormon Point, respectively, above elevations −46 m and −30 m respectively. An MIS 6 age for Beatty bar is also consistent with the faunal ostracod data indicating a saline lake during MIS 2 (Forester et al., 2005).

Like the Beatty bar, the Manly shorelines dates may be interpreted as either MIS 2 or MIS 6. However, the Manly shorelines have the oldest date for any Lake Manly-related deposits at ~465 ka. The Manly shorelines at an altitude of ~10 m below sea level are significantly lower than the Beatty Junction bar complex, which lies at ~45 m asl. Assuming the Beatty Junction bar complex was formed during MIS 2, the Manly shorelines would have been intermittently covered by water during MIS 2 according to Anderson and Wells (2003). Consequently, the surface of the Manly shorelines would have been reworked by wave action. This suggests that the clasts that were dated using ^{10}Be TCN methods on the Manly shorelines were reworked from the previous MIS 6 high stand and/or slope debris and had significant prior exposure.

Alternatively, if the Beatty bar has a MIS 6 age, the mean TCN ^{10}Be date of 209 ± 142 ka at the Manly shorelines is consistent with clasts having variable amounts of inherited ^{10}Be deposited in an MIS 6 lake. This interpretation is consistent with observations by Machette et al. (2008) and Knott et al. (2002, 2004) that the MIS 4 and MIS 2 lake shorelines never rose above −46 m and −30 m, respectively. This is also consistent with the interpretation by Forester et al. (2005) that the MIS 2 lake was a saline mudflat and not a freshwater lake.

In sedimentary environments where reworking of material is common, such as deltas, the youngest dates are generally considered to be the best indicator of the age of the deposit (Stanley and Hait, 2000; Knott and Eley, 2006). If this practice is applied to the TCN ^{10}Be dates at the Beatty bar and Manly shorelines, the interpreted TCN ages of these deposits would be ~119 ka and ~109 ka, respectively.

Machette et al. (2008) used a ^{36}Cl depth profile to date a lacustrine delta complex on Hanaupah Canyon fan west of Badwater to ~130 ka, which is consistent with deposition during a high stand of Lake Manly at the end of MIS 6. The dated deposits are at an altitude of ~30 m asl, which relates to a lake with a maximum depth of ~115 m. Machette et al. (2008) also showed that remnants of shoreline deposits that are present at higher elevations (>67 m asl) on the southern margin of the Hanaupah Canyon fan complex are cut across older alluvium and may be related to an MIS 6 or, more likely, an MIS 8 or earlier high stand.

Our results highlight the problems of using surface clasts to date landforms in Death Valley, and underscore the potential problems of applying such methods in other similar semi-arid and arid settings where there is significant prior exposure and slow sediment transfer. Armstrong et al. (2010) showed similar problems for piedmont mountain front deposits along the eastern Sierra El Mayor in northern Baja California. Despite the potential problems of using TCN dating of surface cobble and boulders to define ages on alluvial fan surfaces in Death Valley, a combination of TCN surface and depth-profile methods, along with other Quaternary dating techniques, such as OSL geochronology, may provide useful determinations of landform

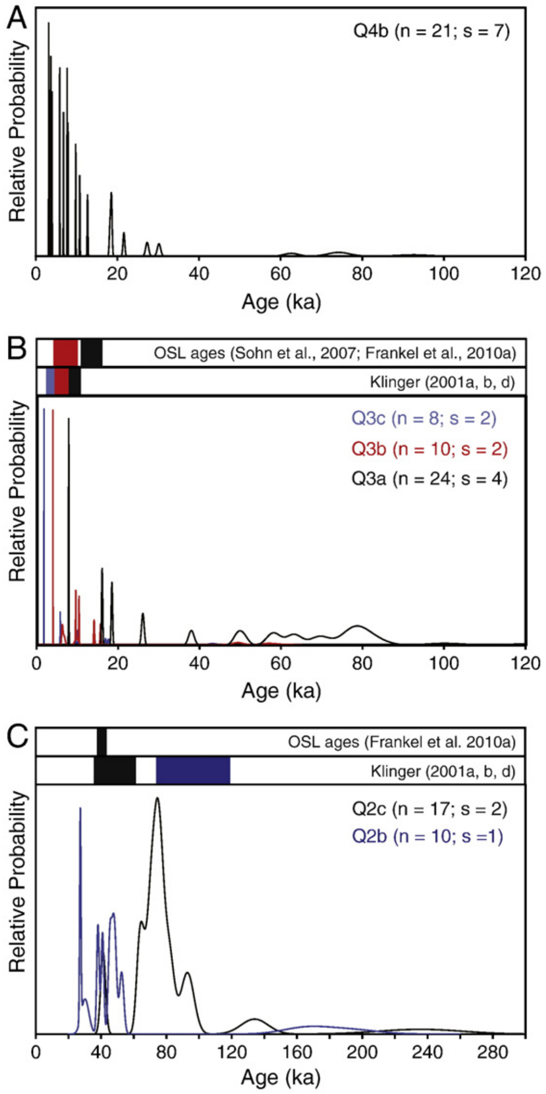

Fig. 10. Probability distribution plots for ^{10}Be TCN ages for A) Q4b, B) Q3a, Q3b, Q3c and C) Q2a and Q2b units. The number of samples and number of locations used in each probability plot is highlighted by n and s, respectively. Klinger (2001a,b,d) estimates of surface ages and OSL ages are highlighted by the bars above the probability plots (colors refer to surface ages highlighted by the color of the text for n and s). Q4b are samples BWF082, 083, 084 and 085, and Bwater6, 7 and 8 from Frankel et al. (2010b) for active channels south of Badwater; and samples Q3a are from from Mud Canyon including samples KF-0416-1 to 6 and Sc1A, B, C, and from Frankel et al. (2010a) samples DVFC1A to E and KF-0506-1 to 10. Q3b are from samples DVFC2A, C, D and E from South Junction; and from Frankel et al. (2010b) including samples KFMP-101, 103, 105, 106, 110 and 112 from Mormon point. Q3c are from Badwater fans including samples Bwater1 to 5 and BWF086, 088 and 089 from Frankel et al. (2010b). Q4a are samples from North Junction and Big Dip Canyon, and include samples Sc5A and B, and Sc6A, B and C, respectively. Sc2a and B, Sc3A, B and C, and Sc4A and B from Frankel et al. (2010a) for active channel in the Mud Canyon area. Q2b are samples KF-0218-2, 3, 4 and10, and KF-0404-1 to 6 from North of Ubehebe Crater.

age to investigate tectonic rates and other processes in this region (e.g., Frankel et al., 2007a, 2010a,b). Moreover, the TCN ages provide important information, which when used in combination with other geochronological methods, provide significant insights into the processes that operate on alluvial fans and associated landforms in drylands. Application of TCN methods to cobbles and boulders on surfaces in drylands, therefore, may be more useful and valuable as a process tool in these environments rather than for simply dating a surface.

8. Conclusions

The ^{10}Be TCN ages from individual alluvial fan surfaces in Death Valley show considerable variance. In particular, samples collected in the active channels date from ~6 ka to ~93 ka. This shows that there is significant inheritance of ^{10}Be TCN in clasts that ultimately form alluvial fans in Death Valley, which is likely on the order of 10^3 to 10^4 years. This is probably because bedrock hillslopes erode slowly and clasts reside in channels and flood-plains for long periods in this semi-arid to arid region; hence, this material is exposed to cosmic rays and acquires a component of inherited TCNs. Comparisons of ^{10}Be TCN ages on alluvial fan surfaces with chronostratigraphies based on soil development and OSL dating show that minimum ^{10}Be TCN ages within sample sets on individual surfaces more closely approximate the age of the surface for landforms younger than ~70 ka. However, alluvial fan surfaces older than ~70 ka have undergone significant erosion such that the majority of ^{10}Be TCN ages for datasets on individual surfaces underestimate the true age of the surface due to erosion and exhumation of fresh clasts.

The ^{10}Be TCN ages for Beatty Junction bar complex and the Manly shorelines range from ~119 ka to ~385 ka and ~109 ka to ~465 ka, respectively. The youngest dates may represent the age of the deposit, as is frequently the case in reworked deposits, and many clasts have a substantial inherited ^{10}Be TCN. An MIS 6 age for these deposits, based on the younger ages, is consistent with mapping and dating by Machette et al. (2008) at the Hanaupah Canyon fan as well as mapping and observations at Mormon Point (Knott et al., 2002, 2004), hydrologic modeling (Matsubara and Howard, 2009) and faunal interpretation of the Badwater core (Forester et al., 2005). This suggests that OSL dates of ~19 ka (Table 3) record deposition of younger elluviated materials. However, the new OSL and previously published and preliminary OSL and TL ages and soil development allow interpretation that these landforms formed during MIS 2 (~22–18 ka). The disparity between dates determined by different dating methods and the large spread of TCN ages suggests that the cobbles and boulders have considerable inherited ^{10}Be concentrations and implies that the clasts have been derived from older shorelines or associated landforms.

Our results highlight the significant problems associated with using surface cobbles and boulders to date surfaces using ^{10}Be methods in Death Valley and probably for other similar semi-arid and arid settings. We suggest that a combination of TCN surface and depth profile methods, together with other techniques such as OSL dating and geologic mapping, are needed to accurately determine late Quaternary landform chronologies in semi-arid environments such as Death Valley. The application of TCN methods to alluvial fans and similar landforms when used in combination with other geochronological methods has the potential to provide important insights into the processes that operate on alluvial fans and associated landforms in drylands. These studies are clearly essential for a variety of tectonic, geomorphic, paleoenvironmental, landscape development and archaeological research.

Acknowledgements

This study was supported by National Science Foundation grants EAR-0537580 (Owen), EAR-0537901 (Dolan) and EAR-0538009 (Finkel), a NASA Earth System Science Fellowship (Frankel), a LLNL-UEPP Fellowship (Frankel), Georgia Institute of Technology (Frankel), and the Geological Society of America (Frankel). Alicia Nobles is thanked for her help with sample preparation. Thanks to Andrew Plater and an anonymous reviewer for their constructive and useful comments on our paper. LiDAR data were collected by NCALM and are

Table 6
Summary of ^{10}Be ages for surfaces in this study and Frankel et al. (2007a,b, 2010a,b) and OSL ages.

	Quaternary stratigraphic units after Klinger (2001a) and Frankel and Dolan (2007)	Estimated ages after Klinger (2001a)	OSL ages for surfaces after Frankel et al. (2010a,b)	OSL ages for surfaces after Sohn et al. (2007)	^{10}Be ages Range, and mean and standard deviation
Holocene	Q4b	Historic			2.0–92.6 ka 24.4 ± 27.2 ka
	Q4a	0.2–2 ka			
	Q3c	2–4 ka			1.8–88.0 ka 24.6 ± 28.5 ka
	Q3b	4–8 ka	3.2–8.0 ka (Mormon Point and Badwater)	4–10 ka	4.0–57.1 ka 18.3 ± 18.8 ka
	Q3a	8–12 ka	14–21 ka (Mud Canyon)	11–17 ka	7.6–152.6 ka 68.6 ± 35.4 ka
				Q2d: 25–26 ka	
Pleistocene	Q2c	35–60 ka	~38 ka (Mud Canyon)		41.3–235.5 ka 87.8 ± 43.8 ka
	Q2b	80–120 ka			27.3–191.1 ka 68.6 ± 58.5 ka
	Q2a	>180 ka			

based on services provided by the Plate Boundary Observatory operated by UNAVCO for EarthScope and supported by the NSF (EAR-0350028 and EAR-0732947).

References

Adamiec, G., Aitken, M., 1998. Dose-rate conversion factors: update. Ancient TL 16, 37–50.

Anderson, D.E., 1998. Late Quaternary paleohydrology, lacustrine stratigraphy, fluvial geomorphology, and modern hydroclimatology of the Amargosa River Death Valley hydrologic system, California and Nevada: Riverside, California, University of California Riverside, unpublished Ph.D dissertation (521 pp.).

Anderson, D.E., Wells, S.G., 2003. Latest Pleistocene lake highstands in Death Valley, California. In: Enzel, Y., Wells, S.G., Lancaster, N. (Eds.), Paleoenvironments and paleohydrology of the Mojave and southern Great Basin Deserts. Geological Society of America Special Paper 368, pp. 115–128.

Armstrong, P., Perez, R., Owen, L.A., Finkel, R.C., 2010. Timing and controls on late Quaternary landscape development along the eastern Sierra el Mayor, northern Baja California, Mexico. Geomorphology 114, 415–430.

Balco, G., Stone, J.O., Lifton, N.A., Dunai, T.J., 2008. A complete and easily accessible means of calculating surface exposure ages or erosion rates from ^{10}Be and ^{26}Al measurements. Quaternary Geochronology 8, 174–195.

Birkeland, P., 1999. Soils and Geomorphology. Oxford University Press, Oxford. (448 pp.).

Blackwelder, E., 1933. Lake Manly: an extinct lake of Death Valley. Geographical Review 23, 464–471.

Brogan, G.E., Kellogg, K.S., Slemmons, D.B., Terhune, C.L., 1991. Late Quaternary faulting along the Death-Valley Furnace Creek fault system. U.S. Geological Survey Bulletin, California and Nevada. 1991 (23 pp.).

Budahn, J.R., Wandless, G.A., 2002. Instrumental neutron activation by abbreviated count: U.S. Geological Survey Open-File Report 02-223, Chapter X, on-line only at http://pubs.usgs.gov/of/2002/ofr-02-0223/.

Bull, W.B., 1968. Alluvial-fans. Journal of Geological Education 16, 101–106.

Bull, W.B., 1991. Geomorphic Responses to Climate Change. Oxford University Press, New York. 326 pp.

Burchfiel, B.C., Stewart, J.C., 1966. "Pull-apart" origin of the central segment of Death Valley, California. Geological Society of America Bulletin 77, 439–442.

Burchfiel, B.C., Molnar, P., Zhang, P., Deng, Q., Zheng, W., Wang, Y., 1995. Example of a supradetachment basin within a pull-apart tectonic setting: Mormon Point, Death Valley, California. Basin Research 7, 199–214.

Denny, C.S., 1965. Alluvial fans in the Death Valley region, California and Nevada. U.S. Geological Survey Professional Paper 466, 62 p., with 5 plates.

Dorn, R.I., 1988. A rock varnish interpretation of alluvial-fan development in Death Valley, California. National Geographic Research 4, 56–73.

Forester, R.M., Lowenstein, T.K., Spencer, R.J., 2005. An ostracode based paleolimino-logic and paleohydrologic history of Death Valley: 200 to 0 ka. Geological Society of America Bulletin 117. doi:10.1130/B25637.1.

Frankel, K.L., Dolan, J.F., 2007. Characterizing arid region alluvial fan surface roughness with airborne laser swath mapping digital topographic data. Journal of Geophysical Research 112, F02025. doi:10.1029/2006JF000644.

Frankel, K.L., Brantley, K.S., Dolan, J.F., Finkel, R.C., Klinger, R.E., Knott, J.R., Machette, M.N., Owen, L.A., Phillips, F.M., Slate, J.L., Wenicke, B.P., 2007a. Cosmogenic ^{10}Be and ^{36}Cl geochronology of offset alluvial fans along the northern Death Valley fault zone: implications for transient strain in the eastern California shear zone. Journal of Geophysical Research 112, B06407. doi:10.1029/2006JB004350.

Frankel, K.L., Dolan, J.F., Finkel, R.C., Owen, L.A., Hoeft, J.S., 2007b. Spatial variations in slip rate along the Death Valley-Fish Lake Valley fault system determined from LiDAR topographic data and cosmogenic ^{10}Be geochronology. Geophysical Research Letters 34, LI8303. doi:10.1029/2007GL030549.

Frankel, K.L., Dolan, J.F., Owen, L.A., Ganev, P., Finkel, R.C., 2010a. Spatial and temporal constancy of seismic strain release along an evolving segment of the Pacific-North America plate boundary. Earth and Planetary Science Letters, in review.

Frankel, K.L., Owen, L.A., Dolan, J.F., Knott, J.R., Finkel, R.C., Hatfield, J., Masklewixz, T., 2010b. Timing and rates of Holocene normal faulting along the Black Mountain Fault zone, Death Valley. Geological Society of America Bulletin, in review.

Galvin, C., Klinger, R.E., 1996. Lake Manly beach ridges at Beatty Junction, Death Valley, California: Geological Society of America, 28th annual meeting. Abstracts with Programs 28, 458.

Ganev, P.N., Dolan, J.F., Frankel, K.L., Finkel, R.C., 2010. Rates of extension along the Fish Lake Valley fault and transtensional deformation in the Eastern California shear zone–Walker Lane belt. Lithosphere 2, 33–49. doi:10.1130/L51.1.

Gilbert, G.K., 1890. "Lake Bonneville." U.S. Geological Survey Monograph 1.

Hamilton, W., 1988. Detachment faulting in the Death Valley region, California and Nevada, U.S. Geological Survey Bulletin 1790, 763–771.

Hooke, R. LeB, 1972. Geomorphic evidence for late-Wisconsin and Holocene tectonic deformation, Death Valley, California. Geological Society of America Bulletin 83, 2073–2098.

Hooke, R. LeB, Dorn, R.I., 1992. Segmentation of alluvial fans in Death Valley, California—new insights from surface-exposure dating and laboratory modeling. Earth Surface Processes and Landforms 17, 57–574.

Howard, A.D., Selby, M.J., 1994. Rock slopes. In: Abrahams, A., Parsons, A. (Eds.), Geomorphology of Desert Environments. Chapman & Hall, London, pp. 123–172.

Hunt, C.B., Mabey, D.R., 1966. Stratigraphy and structure of Death Valley, California: U.S. Geological Survey Professional Paper 494–A, 162 p., 3 plates (plate 1, 1:96, 000 scale).

Jayko, A.S., 2005. Late Quaternary denudation, Death and Panamint Valleys, eastern California. Earth Science Reviews 73, 271–289.

Klinger, R.E., 2001b. Evidence for large dextral offset near Red Wall Canyon. In: Machette, M.N., Johnson, M.L., Slate, J.L. (Eds.), Quaternary and late Pliocene geology of the Death Valley region: recent observations on tectonics, stratigraphy, and lake cycles. US Geological Survey Open-File Report 01–51, 32–37.

Klinger, R.E., 2001c. Beatty Junction bar complex. In: Machette, M.N., Johnson, M.L., Slate, J.L. (Eds.), Quaternary and late Pliocene geology of the Death Valley region: recent observations on tectonics, stratigraphy, and lake cycles. US Geological Survey Open-File Report 01–51, 40–49.

Klinger, R.E., 2001d. North Death Valley. In: Machette, M.N., Johnson, M.L., Slate, J.L. (Eds.), Quaternary and late Pliocene geology of the Death Valley region: recent observations on tectonics, stratigraphy, and lake cycles. US Geological Survey Open-File Report 01–51, 5–20.

Klinger, R.E., 2001a. Quaternary stratigraphy, soil geomorphology, and tephrochronol-ogy of northern Death Valley—Implications for tectonic activity along the northern Death Valley fault zone: Boulder Colorado, University of Colorado, unpublished Ph. D dissertation.

Klinger, R.E., Piety, L.A., 2001. Holocene faulting and slip rates along the Black Mountain fault zone near Mormon Point. In: Machette, M.N., Johnson, M.L., Slate, J.L. (Eds.), Quaternary and late Pliocene geology of the Death Valley region: recent observations on tectonics, stratigraphy, and lake cycles. US Geological Survey Open-File Report 01–51, 193–203.

Knott, J.R., 1998. Late Cenozoic tephrochronology, stratigraphy, geomorphology, and neotectonics of the western Black Mountains piedmont, Death Valley, California—Implications for the spatial and temporal evolution of the Death Valley fault zone: Riverside, California, University of California—Riverside, unpublished Ph.D. disser-tation, 407 pp.

Knott, J.R., Eley, D.S., 2006. Early to middle Holocene coastal dune and estuarine deposition, Santa Maria Valley, California. Physical Geography 27, 127–136.

Knott, J.R., Tinsley, J.C., Wells, S.G., 2002. Are the benches at Mormon Point, Death Valley, California, USA, scarps or strandlines? Quaternary Research 58, 352–360.

Knott, J.R., Tinsley, J.C., Wells, S.G., 2004. Letter to the Editor. Quaternary Research 61, 344–347.

Knott, J.R., Sarna-Wojcicki, A., Machette, M.N., Klinger, R.E., 2005. Upper Neogene stratigraphy and tectonics of Death Valley—a review. Earth-Science Reviews Special Issue 73, 245–270.
Ku, T.L., Luo, S., Lowenstein, T.K., Li, J., Spencer, R.J., 1998. U-series chronology of lacustrine deposits in Death Valley, California. Quaternary Research 50, 261–275.
Lal, D., 1991. Cosmic ray labeling of erosion surfaces: in situ nuclide production rates and erosion models. Earth and Planetary Science Letters 104, 429–439.
Li, J., Lowenstein, T.K., Brown, C.B., Ku, T.L., Luo, S., 1996. A 100 ka record of water tables and paleoclimates from salt cores, Death Valley, California. Palaeogeography, Palaeoclimatology, Palaeoecology 123, 179–203.
Lowenstein, T.K., Li, J., Brown, C.B., Roberts, S.M., Ku, T.L., Luo, S., Yang, W., 1999. 200 k.y. paleoclimate record from Death Valley salt core. Geology 27, 3–6.
Machette, M.N., Johnson, M.L., Slate, J.L., 2001. Quaternary and Late Pliocene Geology of the Death Valley Region: Recent Observations on Tectonics, Stratigraphy, and Lake Cycles (Guidebook for the 2001 Pacific Cell—Friends of the Pleistocene Fieldtrip). USGS Open-File Report 01–51.
Machette, M.N., Slate, J.L., Phillips, F.M., 2008. Terrestrial cosmogenic-nuclide dating of alluvial fans in Death Valley, California. USGS Professional Paper 1755.
Matsubara, Y., Howard, A.D., 2009. A spatially explicit model of runoff, evaporation, and lake extent: Application to modern and late Pleistocene lakes in the Great Basin region, western United States. Water Resources Research 45, doi:10.1029/2007WR005953.
McFadden, L.D., Ritter, J.B., Wells, S.G., 1989. Use of multiparameter relative-age methods for age estimation and correlation of alluvial-fan surfaces on a desert piedmont, eastern Mojave Desert, California. Quaternary Research 32, 276–290.
McFadden, L.D., Bull, W.B., Wells, S.G., 1991. Stratigraphy and geomorphology of Quaternary piedmont deposits. In: Morrison, R.B. (Ed.), Quaternary Nonglacial Geology: Conterminous US: Geology of North America. Geological Society of America, Boulder, CO, pp. 327–331.
Means, T.H., 1932. Death Valley. Sierra Club Bulletin 17, 67–76.
Mejdahl, M., 1979. Thermoluminescence Dating: Beta Dose attenuation in quartz grains. Archaeometry 21, 61–71.
Miller, M.B., Pavlis, T.L., 2005. The Black Mountain turtlebacks: Rosetta stones of Death Valley tectonics. Earth Science Reviews 73, 115–138.
Moring, B., 1986. Reconnaissance surficial geologic map of northern Death Valley, California and Nevada: United States Geological Survey, Miscellaneous Field Studies Map MF-1770, 1 plate, scale 1:62, 500.
Murray, A.S., Wintle, A.G., 2000. Luminescence dating of quartz using an improved single-aliquot regenerative-dose protocol. Radiation Measurements 32, 57–73.
Nishiizumi, K., Kohl, C.P., Arnold, J.R., Dorn, R., Klein, J., Fink, D., Middleton, R., Lal, D., 1993. Role of in situ cosmogenic nuclides ^{10}Be and ^{26}Al in the study of diverse geomorphic processes. Earth Surface Processes and Landforms 18, 407–425.
Nishiizumi, K., Imamura, M., Caffee, M.W., Southon, J.R., Finkel, R.C., McAninch, J., 2007. Absolute calibration of Be-10 AMS standards. Nuclear Instruments and Methods in Physics Research. Section B: Beam Interactions with Materials and Atoms 258, 403–413.
Nobel, L.F., 1926. Note on a colemanite deposit near Shoshone, California, with a cketch of the geology of part of Amargosa valley. US Geological Survey Bulletin 785, 63–73.
Orme, A.J., Orme, A.R., 1991. Relict barrier beaches as paleoenvironmental indicators in the California desert. Physical Geography 12, 334–346.
Owen, L.A., Robinson, R., Benn, D.I., Finkel, R.C., Davis, N.K., Yi, C., Putkonen, J., Li, D., Murray, A.S., 2009. Quaternary glaciation of Mount Everest. Quaternary Science Reviews 28, 1412–1433.
Perron, J.T., Kirchner, J.W., Dietrich, W.E., 2009. Formation of evenly spaced ridges and valleys. Nature 460, 502–505.
Phillips, F.M., Zreda, M.G., 1999. Chlorine-36 ages of pluvial shoreline features in the Death Valley/Panamint Valley area, in Slate, J.L., ed., Proceedings of Conference on Status of Geologic Research and Mapping, Death Valley National Park: U.S. Geological Survey Open-File Report 99–153, p. 117.
Pigati, J.S., Lifton, N.A., 2004. Geomagnetic effects on time-integrated cosmogenic nuclide production with emphasis on in situ ^{14}C and ^{10}Be. Earth and Planetary Science Letters 226, 193–205.
Poage, M.A., Chamberlain, C.P., 2002. Stable isotopic evidence for a Pre-Middle Miocene rain shadow in the western Basin and Range: Implications for the paleotopography of the Sierra Nevada. Tectonics 21, 1034. doi:10.1029/2001TC001303.
Prescott, J.R., Hutton, J.T., 1988. Cosmic ray and gamma ray dosimetry for TL and ESR. Nuclear Tracks and Radiation Measurements 14, 223–230.
Professional Soil Scientists Association of California, 1998. Interconnectivity and relationships between soil science, geomorphology, geology and paleoclimatology. Annual Meeting, March 5–8. Furnace Creek Ranch Resort, Death Valley. 111 pp.
Reynolds, M.W., 1969. Stratigraphy and structural geology of the Titus and Titanothere Canyons area, Death Valley, California: Berkeley, California, University of California—Berkeley, unpublished Ph. D. dissertation (310 pp.).
Seong, Y.B., Owen, L.A., Bishop, M.P., Bush, A., Clendon, P., Copland, P., Finkel, R., Kamp, U., Shroder, J.F., 2007. Quaternary Glacial History of the Central Karakoram. Quaternary Science Reviews 26, 3384–3405.
Small, E.E., Anderson, R.S., Repka, J.L., Finkel, R.C., 1997. Erosion rates of alpine bedrock summit surfaces deduced from in situ Be-10 and Al-26. Earth and Planetary Science Letters 150, 413–425.
Sohn, M.F., Mahan, S.A., Knott, J.R., Bowman, D.D., 2007. Luminescence ages for alluvial-fan deposits in Southern Death Valley: Implications for climate-driven sedimentation along a tectonically active mountain front. Quaternary International 166, 49–60.
Soil Survey Division Staff. 1993. Soil survey manual. Soil Conservation Service. U.S. Department of Agriculture Handbook 18.
Staiger, J., Gosse, J., Toracinta, R., Oglesby, B., Fastook, J., Johnson, J.V., 2007. Atmospheric scaling of cosmogenic nuclide production: climate effect. Journal of Geophysical Research 112, B02205. doi:10.1029/2005JB003811.
Stanley, D.J., Hait, A.K., 2000. Deltas, radiocarbon dating, and measurements of sediment storage and subsidence. Geology 28, 295–298.
Stone, J.O., 2000. Air pressure and cosmogenic isotope production. Journal of Geophysical Research 105, 23753–23759.
Troxel, B.W., 1986 (Ed.). Quaternary Tectonics of Southern Death Valley, California: Field Trip Guide, Oct. 31-Nov. 2, 1986, Friends of the Pleistocene, Pacific Cell, Shoshone, California.
Trull, T.W., Brown, E.T., Marty, B., Raisbeck, G.M., Yiou, F., 1995. Cosmogenic ^{10}Be and ^{3}He accumulation in Pleistocene beach terraces in Death Valley, California, U.S.A.: implications for cosmic-ray exposure dating of young surfaces in hot climates. Chemical Geology 119, 191–207.
Wernicke, B., Axen, G.J., Snow, J.K., 1988. Basin and Range extensional tectonics at the latitude of Las Vegas, Nevada. Geological Society of America Bulletin 100, 1738–1757.
Western Regional Climate Center, 2010. Western U.S. Climate Historical Summaries Weather. Desert Research Institute. http://www.wrcc.dri.edu/cgi-bin/cliMAIN.pl?ca2319.
Wright, L.A., Troxel, B.W., 1993. Geologic map of the central and northern Funeral Mountains and adjacent areas, Death Valley. U.S. Geological Survey Miscellaneous Investigation Series, Map I-2305, scale 1:48,000.
Wright, L.A., Troxel, B.W., 1999 (Eds.). Cenozoic Basins of the Death Valley Region. Geological Society of America Special Paper 333.